"This report was prepared as an account of work sponsored by a Department of the Federal Government of Canada. Neither the Federal Government of Canada or any agency thereof, nor any contractor or subcontractor, nor any of their employees, makes any warranty, expressed or implied, or assumes any legal liability or responsibility for any third party's use of or the results of such use of any information, apparatus, product or process disclosed in this report, or represents that its use by such third party would not infringe privately owned rights".

WELD PROCESS DEVELOPMENT FOR FABRICATION OF HEAVY WALL PRESSURE VESSEL

PART 3

BY
B. WRIGHT
BABCOCK & WILCOX CANADA

Work on this project was conducted under the auspices of the Canada Centre for Mineral and Energy Technology, Energy, Mines and Resources, Canada.

DSS FILE NUMBER: 06SQ-23340-5-9022
DSS CONTRACT SERIAL NUMBER: OSQ85-00090
CANMET PROJECT NUMBER:
CANMET SCIENTIFIC AUTHORITY: Dr. J.T. McGrath

62 pp

B&W Canada makes no warranty or representation, expressed or implied, with respect to the accuracy, completeness, or usefulness of the information contained in this report or that the use of any information, apparatus, method, or process disclosed in this report may not infringe privately owned rights.

B&W Canada assumes no liability with respect to the use of, or for damages resulting from the use of any information, apparatus, method, or process disclosed in this report or experimental apparatus furnished with this report.

MICROMEDIA

CONTENTS

		Page
1.0	SUMMARY	1
2.0	INTRODUCTION	1
3.0	PROGRAM OUTLINE	2
3.1	Forming the Shell	2
3.2	Welding the Longitudinal Seam	4
3.3	Quenching and Tempering the Shell Section	6
3.4	Welding the Circumferential Seam	6
3.5	Nondestructive Examination	8
3.6	Sectioning and Testing the N-SAW Seam	9
4.0	RESULTS	10
4.1	Shell Dimensional Changes	10
4.2	Nondestructive Examination Results	11
4.3	Weld Metal Composition	12
4.4	Charpy V-Notch Impact Toughness	13
4.5	Weld Metal Structure	14
5.0	DISCUSSION	15
6.0	CONCLUSIONS	19
7.0	REFERENCES	20

ABBREVIATIONS

AC	Alternating Current
BOP	Bead on Plate
DAC	Distance Amplitude Curve
DCRP	Direct Current, Reverse Polarity
MT	Magnetic Particle Examination
NDE	Nondestructive Examination
N-SAW	Narrow Gap Submerged Arc Welding
PWHT	Post Weld Heat Treatment
Q&T	Quench and Temper
RT	Radiographic Examination
SAW	Submerged Arc Welding
SMAW	Shielded Metal Arc Welding
UT	Ultrasonic Examination

TABLES

TABLE		PAGE
1	Properties of 2¼Cr-1Mo Plate for Shell Fabrication	21
2	Weld Parameters for Longitudinal Seam Test Plate	22
3	Weld Parameters for Longitudinal Seam	23
4	Weld Parameters for Circumferential Seam	24
5	Program for Impact Testing the Circumferential Seam	25
6	Shell Plate Dimensional Changes	26
7	Longitudinal Shrinkage Associated with Circumferential Seam Welding	28
8	Changes in Shell Inside Diameter Associated with Circumferential Seam Welding	29
9	Transverse Shrinkage of Circumferential Seam (Face of Preparation)	30
10	Transverse Shrinkage of Circumferential Seam (75 mm Gauge Marks)	31
11	Chemical Composition of Circumferential Seam	32
12	Charpy V-Notch Impact Results	33
13	Charpy V-Notch Properties at -40°C	36

ILLUSTRATIONS

FIGURE		PAGE
1	Flux Drying Oven UT-40A	37
2	Detail of Circumferential Seam Weld Preparation	38
3	Final Configuration of Circumferential Seam Weld	39
4	Macro Structure of Circumferential Seam Weld	40
5	Test Specimen Removal from Circumferential Seam	41
6	Charpy Test Specimen Removal	42
7	Transverse Shrinkage Across Circumferential Seam	43
8	Contour of Longitudinal Weld Root Cracks	44
9	Charpy V-Notch Transition Curve for N-SAW, 3T/4 Location, Notched at W/4	45
10	Charpy V-Notch Transition Curve for Conventional SAW, 1.6 mm Below the ID Surface, Notched at W/2	46
11	Relationship Between Absorbed Energy and Percent Shear for Weld Metal Charpy Specimens	47
12	Typical Macrostructure of N-SAW Weld Metal	48
13	Bainitic Structure in Area 1, 3/4T	49
14	Bainitic Structure in Area 2, 3/4T	50
15	Bainitic Structure in Area 3, 3/4T	51
16	Fracture Appearance of Specimen 83	52
17	Fracture Appearance of Specimen 73	53
18	Fracture Appearance of Specimen 10S	54
19	Fracture Appearance of Specimen 12S	55
20	Microhardness Survey T/4 Location	56
21	Microhardness Survey T/2 Location	56
22	Microhardness Survey 3T/4 Location	57
23	Microhardness Survey 1.6 mm from Surface	57

1.0 RÉSUMÉ

On a fabriqué une section de récipient sous pression de 1,83 m de diamètre intérieur à partir d'une plaque de 2¼Cr-1Mo de 203 mm d'épaisseur en utilisant le système Esab HNG de soudage avec faible écartement des bords pour souder le joint circonférentiel. Les méthodes utilisées pour souder les joints longitudinal et circonférentiel ont donné des soudures qui satisfaisaient aux critères d'examen non destructif de la Division 2, Section VIII, du ASME B&PV Code. Des comparaisons sont faites entre l'utilisation de 2¼Cr-1Mo et l'utilisation d'acier au C-Mn pour la fabrication de sections de récipients sous pression.

On a évalué la distribution de résilience Charpy V à l'intérieur du joint circonférentiel produit par soudage avec faible écartement des bords, et on a montré que la zone de plus faible résilience absorbait à la rupture 54 J à -40 °C.

1.0 SUMMARY

A 1.83 m inside diameter pressure vessel section has been fabricated from 203 mm thick 2¼Cr-1Mo plate using the Esab HNG Narrow Gap Welding System to weld the circumferential seam. Procedures used for the longitudinal and circumferential seams provided welds that were acceptable to the nondestructive examination requirements of ASME B&PV Code, Section VIII, Division 2. Comparisons are made between the fabrication of 2¼Cr-1Mo and C-Mn steel pressure vessel sections.

The Charpy V-Notch toughness distribution within the Narrow Gap welded circumferential seam has been evaluated and the area of lowest toughness has been shown to meet 54J at -40°C.

2.0 INTRODUCTION

Pressure vessels for processing fuel from conventional and tarsands resources involves fabrication of heavy wall thickness 2¼Cr-1Mo material. Canadian fabricators are restricted by the availability of forged shell sections to produce these vessels so that the use of formed plate to manufacture shell sections requires evaluation. Narrow gap welding processes have been developed to effectively weld heavy wall thicknesses but the evaluation of the narrow gap submerged arc welding process for welding 2¼Cr-1Mo steel has in Canadian research work been limited to a laboratory scale.

The purpose of this program was to compare fabrication techniques for the manufacture of a shell section from 2¼Cr-1Mo plate with those for forming C-Mn plate and to evaluate the use of the Esab AB HNG Narrow Gap system for submerged arc welding circumferential seams in a production environment.

The program involved the following tasks:

1. Manufacture of a 1.83 m wide x 1.83 m inside diameter shell by roll forming a 203 mm thick plate, welding of and nondestructive examination of the longitudinal seam followed by quenching and tempering of the assembly.

2. Preparation of a circumferential seam by narrow gap submerged arc welding and the evaluation of weld groove shrinkage. The seam was subjected to the nondestructive examination requirements of ASME Boiler and Pressure Vessel Code, Section VIII, Division 2 both before and after typical reactor vessel post-weld heat treatments.

3. Evaluation of the Charpy V-Notch toughness distribution in the circumferential seam and correlation of the properties with weld metal chemistry and microstructure.

3.0 PROGRAM OUTLINE

3.1 Forming the Shell

Fabrication of pressure vessels from heavy wall 2¼ Cr-1 Mo plate involves hot forming of the material into shell sections followed by a quench and temper (Q&T) to develop the properties specified for ASME SA387 Gr22 Cl.2. Longitudinal welds are made either prior to or after Q&T. Circumferential welds are made with subsequent post weld heat treatment (PWHT) only. For this project, the plate sections were formed in one piece with the longitudinal seam welded prior to Q&T; this shell was then flame cut into two pieces to prepare the circumferential weld seam.

The 6.6 m long x 1.83 m wide x 203 mm thick SA387 Gr22 Cl.2 plate was ordered in the as-rolled and tempered condition to produce the 1.83 m inside diameter (ID) shell section. Chemical analysis and mechanical properties of the plate after a Q&T and simulated PWHT are recorded in Table 1.

Heavy plate is formed at Babcock & Wilcox Canada using a Wilhelmsburger DWVH 3660/120 three roll, plate bending machine. This equipment is capable of roll forming 203 mm thick plate at 3.6 m width. As with all three roll pinch type machines, flat areas remain unbent at both ends of the plate after rolling. To minimize the length of unbent plate ends and, therefore, the amount of plate to be discarded, the ends are preformed to match the shell inside diameter. This preform or crimping operation is made by holding the plate ends between the top stationary roll and one of the bottom rolls whilst the second bottom roll is raised to bend the plate end around the top roll. Some loss of plate length is still necessary to maintain roundness tolerances. The ordered plate length exceeds the nominal circumferential plate length by a standard amount equal to a single plate thickness to compensate for trimming off the flat ends. The ordered plate length was therefore 6.38 m + 203 mm = 6.59 m minimum. The end of the plate entering the rolls is used to align the plate square to the rolls and is cut square with the plate length to avoid excessive trimming at the circumferential seam weld preparations. The normal allowance of one plate thickness over the nominal width was applied for edge trimming.

Roll forming of 203 mm thick plate is performed at the normalize temperature in two stages. The first stage heating is followed by crimping the plate ends and partially forming the cylinder. After the longitudinal weld preparation has been cut the plate is reheated and rolled to bring the plate ends together to form the root gap of the weld preparation. Loss in plate thickness resulting from oxidation during the two heating cycles is normally 3 mm for Carbon-manganese steels and the same compensation was used for the 2¼ Cr-1 Mo plate even though the forming temperatures recommended by Creusot-Marrel were higher than for the C-Mn steel.

The method of hot forming outlined above requires the plate ends to be flame cut to give the 5° side wall angle and the 22 mm root gap for the longitudinal weld preparation prior to completion of the second stage roll. Deformation of the plate requires consideration in two areas so that the longitudinal seam weld preparation can be accurately located and cut. Firstly, the plate does not deform uniformly across the plate width; elongation is greater at the plate mid-width. Without correction the weld preparation would become narrow at the mid-length. The flame cut of the plate ends prior to second stage rolling is, therefore, made as a curve to compensate for this non-uniform plate elongation. Secondly, only the neutral axis of the shell plate maintains the nominal circumferential length; the non-uniform flow through the thickness requires compensation in order that a 5° side wall will result after the second stage roll.

A further consideration during roll bending is the effect of the non-uniform deformation through the thickness upon the plate edge contour. During forming the increase in plate width and length at the inside surfaces is compensated by a contraction at the outside surfaces. The effect (Table 6) is to both reduce the thickness at the shell edges and to increase the shell diameter locally as the material flares outward. The practical significance is greatest for the shell edges because it will govern how much material needs to be trimmed at the circumferential weld preparation.

The plate was dimensionally inspected for width and thickness prior to and after rolling; the average values are recorded in Table 6. The flat plate was uniformly heated to 995°C (1825°F) held for 4 h, 15 min., removed from the furnace and crimped at both ends; the degree of crimping was monitored with a template to match the final outside diameter. The plate was then rolled to an incomplete cylinder with a gap of approximately 750 mm between the plate ends. After the cylinder had cooled to room temperature, the profile for the longitudinal weld preparation was laid out and flame cut with reference to the shell mean circumference; this operation also removed the short unbent plate remaining after crimping. The weld preparation side walls were then ground and subjected to magnetic particle examination with acceptable results. The partial cylinder was reheated to 995°C, held for 4 h 15 min. and then re-rolled to match the OD template and to give the 22 mm root gap required for the longitudinal seam. The offset at the longitudinal seam was adjusted and the root gap was set by welding chordal stays across both ends of the shell prior to the shell cooling to room temperature. The cylinder was measured for inside diameter at eight equally spaced locations and for root gap at six equally spaced locations along the longitudinal seam. The extent of flare-out was measured at four locations at both edges of the shell. The results of these inspections are recorded in Table 6.

3.2 Welding the Longitudinal Seam

Comparative tests of submerged arc welds in 2¼ Cr-1Mo steel have shown that weld metal deposited with AC current exhibits higher toughness than weld metal deposited with DCRP current (1) (2). One reason for such improvement in toughness has been attributed to improved Carbon retention with AC welding (1) and increased Carbon levels have been considered as beneficial in reducing the variation in toughness across narrow gap joints (3) (4).

Preliminary AC welding tests were made using a 150 mm thick assembly with the consumables previously identified as providing high toughness values (4). Conventional AC welding equipment (Linde CAC 1200 Power Source and Lincoln NA4 feeder/controller) was used to confirm welding parameters. The test weld initially showed porosity in the third layer of deposit at which time welding was stopped and the causes of porosity investigated. The Thyssen UV420TTR agglomerated flux had been dried at 230°C, a conditioning previously proven acceptable (4). Welding parameters were varied independently (500 to 700A, 30 to 34V and flux burden from 25 to 38 mm) but porosity persisted during Bead on Plate (BOP) tests.

The flux used for these test welds had been dried in a Gullco Flux Holding Hopper which features two rows of heating elements through the height of the flux. Temperature measurements through the flux height showed a variation of 230°C to 550°C with the oven set at a nominal 230°C (at the base of the container) i.e., the flux had been exposed to temperatures above the manufacturer's recommendation for baking at 350°C. Flux of the same lot number from an unopened bag was baked in the same oven at 230°C for four hours, the temperature distribution being confirmed with thermocouples located through the depth. BOP tests were porosity free as were subsequent welds in 35 mm thick weld grooves. This flux was then used to weld the 150 mm thick assembly. The second layer of the new weld metal showed porosity. BOP tests with the same flux were welded immediately after this test using a DC power source and showed no porosity.

The flux manufacturer (Thyssen Draht AG) confirmed that the UV420TTR flux used was of their AC formulation and that baking at 350°C for 4h would dry the flux (3). This treatment was applied to batches of flux in 50 mm deep trays in an electric muffle furnace but the 150 mm test assembly welded with AC SAW again showed porosity after two layers. The flux manufacturer also advised (3) that on occasion welding with UV420TTR had resulted in porosity problems with AC SAW although the cause was not clear; in Europe, tandem AC-AC and AC-DC welding is successful with this flux and the manufacturer suggested the use of a Miller CP square wave AC power source to overcome the porosity problem.

In an attempt to rationalize the apparent poor AC current handling capacity of this flux a comparison of power source wave forms was made using Linde 124 flux as a reference during single wire BOP tests.

Neither the amperage nor voltage wave forms monitored on an oscilloscope showed significant differences between the two fluxes. The voltage wave form was in both instances erratic and clipped; the amperage wave form was smoothly sinusoidal. There was no visible evidence to show poor arc initiation during the negative power cycle with the UV420TTR flux and the use of an alternate power source was not pursued.

The cause of porosity in the welds made with UV420TTR flux using an AC power supply was not resolved but the evaluation suggested the need for an improved preconditioning oven for agglomerated fluxes and for an alternative flux for AC welding.

Several welding equipment distributors were contacted for an improved flux drying oven. The Flux Dry Oven UT-40A (Fig. 1) developed by Thyssen Draht engineers was recommended to uniformly precondition agglomerated fluxes. The flux is inserted at the top of the unit and remains until the preset drying temperature is attained; the oven then rocks from side to side causing the warm flux to cascade over a series of shelves until new flux enters the first heating zone. The rocking action stops until the new flux attains the preset temperature and the cycle is repeated until the preconditioned flux falls into the base of the oven where it is collected in removable containers held at a warming temperature. The oven was said to deliver preconditioned flux at a rate of 45 kg/h. The unit purchased for this project was the first exported to Canada; the manufacturer had converted a European model to 575V power supply and only minor modifications were necessary to the control circuitry during laboratory trials. The oven operated successfully for the duration of longitudinal and circumferential seam welding.

Agglomerated fluxes for 2¼ Cr-1Mo welding were reviewed for AC welding the longitudinal seam. Oerlikon OP76 flux had been shown to provide good operating characteristics using conventional, sine-wave AC power sources with both single and tandem arc procedures (5). A 150 mm thick test assembly was welded using the parameters shown in Table 2 without any visible porosity. The test weld was ground and inspected by radiographic examination and found acceptable to ASME B&PV Code, Section VIII, Division 2 requirements.

The 1.83 m longitudinal seam was welded using the parameters listed in Table 3 and the consumables listed in Table 2. After removal of the backing bar by thermal gouging, the seam was ground on both faces using a manipulator mounted belt grinder in preparation for nondestructive examination (NDE). Both faces of the weld were magnetic particle inspected using conventional AC Yoke Methods. Radiographic examination was performed with a 4 MeV Linatron using a sensitivity of 2-1T. Ultrasonic examination was performed with normal beam and angle beam probes to provide complete volumetric inspection. In addition to the ultrasonic examination required by ASME B&PV Code, Section VIII, Div. 2, the seam was also inspected using a tandem probe technique to further

examine the joint side wall (6). The tandem probe inspection used 2¼ MHz, 25 mm dia. transmitter and receiver probes. A 6 mm diameter hole calibration block was used to produce the reference signal.

The longitudinal seam was not mechanically tested as a part of this program.

3.3 Quenching and Tempering the Shell Section

The original intention of the program was to Q&T the shell section to develop weld and base metal properties as one piece but because of weld defects found by NDE (see paragraph 4.2) the shell was cut into two sections through the major defect. Local, Canadian heat treatment vendors were not able to perform the heat treatment so the Q&T was performed by Babcock and Wilcox Co., in Barberton, Ohio. Lifting lugs were welded to each section and both pieces were stress relieved at 690°C for 3h prior to shipping to the heat treatment vendor. The heat treatment cycle is summarized as: heat at 110°C/h to 940° ±14°C and hold for 5h. Quench into water at 38°C max. Heat at 110°C/h to 648° ±14°C and hold for 6h. Air Cool. Upon return to Babcock & Wilcox Canada, the shell sections were shot blasted to remove heat treatment scale and the inside diameters were again measured (Table 6). The longitudinal weld seam was magnetic particle examined and found to be free of defects.

3.4 Welding the Circumferential Seam

The circumferential seam weld preparation was machined using a vertical boring mill to the dimensions shown in Fig. 2. The circumferential seam was welded initially from the outside circumference using N-SAW and the weld root was machined to sound metal using a vertical boring mill. The weld was completed using conventional SAW. This sequence is not the preferred method of circumferential seam manufacture which would involve welding the inside weld preparation with N-SAW or conventional SAW, back grinding the outside weld preparation to sound metal and completing the weld with N-SAW. However, the Esab welding equipment would not practically enter the 1.8 m inside diameter shell and the manipulator mounted, wheel grinder had not been shown capable of following the contour of the narrow gap weld preparation to remove the root of an inside weld.

The two shell sections were fitted with the weld preparation horizontal. This also represents a deviation from preferred manufacturing practice. The circumferential seams of full length shells are fitted with the preparation vertical, adjustments to the fit-up being made using the rotation rollers. The length of the two sections (0.6 and 1.2 m) in this instance were too short to permit normal assembly. The circumferential seam was tack welded at the inside weld preparation using six, 75 mm long

x 19 mm deep block welds welded with SMAW at 150°C preheat. The longitudinal seams in the two sections were rotated 90° apart to give a mismatch in ovality of two adjacent shell cans. The inside surface of the shell was gauged in four locations, 25 mm either side of the weld preparation to monitor lateral shrinkage resulting from welding. Similar reference marks were made at the outside and inside surfaces 305 mm either side of the weld preparation. A partial weld preparation was machined into the outside circumference of the shell. This used to set up the Esab equipment for circumferential seam welding, to confirm weldability of the new flux and then to train welders.

The training of two experienced SAW operators on the Esab system was carried out in two stages. The operators were provided with a manual based on that supplied by Esab and instructed on the use of the equipment in the laboratory with the controller programmed for longitudinal seam welding. The operators then welded a 150 mm thick x 0.9 m long test assembly which was subjected to radiographic examination; this stage of training took three days. Acceptable RT results were obtained on the first test plate. The second stage involved a review of the operating manual two months later and instruction on the use of the equipment programmed for circumferential seam welding. Each operator deposited three beads in the test gap machined into the shell prior to welding the circumferential seam; this stage of training occupied 4 h. The operators found the equipment and controls no more difficult to operate than with conventional SAW machines.

Consideration was given to welding the circumferential seam using the Esab equipment with an AC power source rather than the DC unit initially supplied. The Miller Square Wave AC power source has been used with good results in narrow gaps to weld 2¼ Cr 1-Mo (2). Interfacing the two units was pursued with both manufacturers. The evaluation suggested that the interface was plausible but completing this first of a kind endeavour by coordinating the technologies of a U.S. and a Swedish manufacturer was considered too time consuming. Thyssen Draht suggested that the same end (higher Carbon in the weld) could be achieved by using UV420TTRC flux which was said to compensate for Carbon losses (3). This flux was used for the circumferential seam instead of the UV420TTR flux previously tested (4).

The N-SAW welding equipment was given the complete maintenance program recommended by the manufacturer after it was moved from laboratory to shop location. The control circuit was changed from the longitudinal seam to the circumferential seam mode by substituting one circuit board in the controller (4). The only modification made to the welding head prior to welding the seam was to increase the length of the vertical guidance probe to permit an electrode extension of 41 mm to be obtained.

The outside circumference of the seam was welded by shop welders working 12 h shifts with laboratory staff acting as supervision. Table 4

summarizes weld parameters used together with details of welding consumables. The marginal differences between these parameters and those used for the full thickness sample are the result of differences in weld preparation (4). Amperage values were increased to improve bead appearance and the voltage was decreased from 34V to 32V to improve slag removal; the heat input however was identical to that previously used (4). Preheat was attained using two natural gas burners located either side of the weld preparation at approximately the 7 o'clock position. Consumable usage and welding times were monitored during N-SAW and weld deposition rates calculated from measured wire feed speeds.

The shrinkage across the face of the joint and across gauge marks located 75 mm from the face was measured after each layer. Results are recorded in Tables 9 and 10. Shrinkage did not occur as predicted (4) and three beads per layer were required to fill the joint above the 44th layer.

A shortcoming of the equipment procured was observed during welding the top of the joint. The Esab guidance system is activated by a probe which tracks one side wall of the joint but over the final 25 mm of gap the probe leaves the joint and bead placement is adjusted by the operator. The two shell sections used in this program had been intentionally fitted so that the ovality did not coincide causing the circumferential seam to wander during rotation. The operator was not able to compensate for the oscillating motion of the seam side wall and numerous lack of side wall fusion defects were produced in the top 25 mm of weld. Narrow gap welding was stopped and the joint held for four hours at the preheat temperature prior to cooling to room temperature. The top 28 mm of weld preparation was machined to remove the side wall defects and the inside of the gap was machined to remove the weld root. Both inside and outside surfaces of the joint were completed with conventional SAW using the welding consumables and parameters in Table 4 to produce the final joint configuration shown in Fig. 3.

Transverse shrinkage of the shells was measured between the reference marks at the inside and outside surfaces and the change in inside diameter was measured at four reference points (Tables 6 and 7).

The shell was given a final PWHT cycle at 690°C for 17½h. The time at temperature was selected to represent three cycles of PWHT required by the ASME Code (Table AF-402.1), i.e. one for normal fabrication, one for a repair cycle, and one for field contingency use. The plate thickness was again measured (Table 6).

3.5 Nondestructive Examination

Both surfaces of the weld were conditioned for NDE by grinding with a manipulator mounted belt grinder. The circumferential seam was subjected to magnetic particle, radiographic, and ultrasonic examinations in

accordance with ASME B&PV Code Section VIII, Division 2. The seam was also inspected using a tandem probe ultrasonic test technique to further examine the joint side walls.

After final PWHT, the longitudinal seam was subjected to ultrasonic examination and the circumferential seam was re-examined by magnetic particle, radiographic, and ultrasonic inspections including a repeat tandem probe ultrasonic inspection.

3.6 Sectioning & Testing the N-SAW Seam

The test material from the circumferential seam was removed by flame-cutting prior to PWHT in order to examine the as-welded structure by metallography. The 915 mm long x 230 mm wide test material (115 mm either side of the weld centre line) was post-weld heat treated in the same furnace load as the shell.

The intended program of evaluating the Charpy V-Notch toughness of the N-SAW seam required modification in light of the use of conventional SAW to complete the root and face of the seam. The initial and revised programs of testing are summarized in Table 5. The macro-section was milled, ground, and etched and showed that the N-SAW beads were extremely small (see Figure 4). In an attempt to sample uniform macrostructural areas, the removal of material for preparation of Charpy V-Notch specimens was performed by saw-cutting the cross-sections radially. To facilitate this operation and to maintain the cross-sections perpendicular to the weld axis, the sides of the cut-out were milled parallel to the centre line of the circumferential seam weld within 0.6 mm. The test specimen was laid out radially using the true centre of the section radius and saw-cut to produce wedge shaped blanks (see Fig. 5). These blanks were then milled parallel to the reference face prior to removing the 16 mm square blanks for the Charpy specimens. Positive identification to the surface to be notched, the reference surface in Fig. 5 as indicated by the base of the $\perp$, was maintained during all stages of Charpy specimen machining. The Charpy blanks were milled, ground, etched, and notched to comply with ASTM A370, Figure 11, Type B. Test specimens were cooled to the test temperature using Dry Ice and alcohol and tested in accordance with ASTM A370 using a Tinius Olsen Impact Machine of 195 J capacity.

Samples for chemical analysis were taken with a 6 mm drill along the weld centre line. Samples for Oxygen and Nitrogen analysis were taken as 25 mm square sections 76 and 127 mm beneath the weld outside surface.

Microhardness surveys across the weld gap were conducted at the T/4, T/2 and 3T/4 locations and 1.6 mm from the weld root using a Wilson Tukon Microhardness Machine with a Knoop indenter and 500g load.
Metallographic examination of the weld cross-section was conducted using

optical microscopy. A limited number of broken Charpy specimens were examined using Scanning Electron Microscopy in attempt to rationalize the differences in toughness noted within the gap.

4.0 RESULTS

4.1 Shell Dimensional Changes

The root gap of the longitudinal weld preparation was measured as 24.6 to 26.2 mm compared to the aim of 22 mm and the offset at the preparation was measured at 0.3 mm maximum, i.e. well within the 4.8 mm limit required by the ASME Code (7). The difference between maximum and minimum inside diameters of the shell at any cross-section is not permitted to exceed one percent of the nominal inside diameter (7). The measurements taken after hot forming are recorded in Table 6 and show the maximum difference as 6.4 mm or 0.35% of the nominal diameter. The mean diameter of the shell was measured as 1834.3 mm, i.e. 4.3 mm above the nominal value. Minor dimensional changes occurred as a result of longitudinal welding but the maximum ovality remained at the same position as before welding, i.e. the longitudinal weld did not significantly deform the shell. The increase in ovality noted after quench and temper is not readily explained although an increase in mean diameter might be expected; the position of maximum ovality was not the same as in the welded condition but was still divorced from the longitudinal seam. Although the Code limit for maximum ovality was not violated, had the shell been formed for a pressure vessel it would have been re-rounded after quench and tempering to reduce the ovality below 6 mm in order that the 19 mm maximum offset at the circumferential joints (7) could be met with comfort.

The length of flare out (Table 6) was recorded as 150 mm average at each edge of the shell, i.e. greater than the extra 200 mm material ordered on the width for trimming the edges of the shell at the circumferential weld preparations.

Plate thickness measurements (Table 6) indicate an 8 mm reduction resulting from scaling during heating for hot forming. A further loss of 1.2 mm was recorded after Q&T.

Contraction of the shell resulting from circumferential seam welding after completion with conventional SAW is summarized in Table 7. These measurements were made with a vernier scale between centre punch marks and as such are considered accurate to $\pm$0.4 mm. The results indicate that the longitudinal shrinkage resulting from circumferential seam welding is a maximum of 1.6 $\pm$0.4 mm. Because most of the seam was welded using N-SAW, these results are considered representative of that process. The results after PWHT are inconsistent but suggest a tendency to extend the shell length. Changes in the gauge lengths after Q&T were not

measured because scaling and subsequent shot blasting removed the reference marks.

Circumferential seam welding produced a decrease in the ID of the shell (see Table 8). This decrease was greatest at the weld preparation and negligible at a distance of 310 mm from the seam. The change in diameter resulting from PWHT was negligible.

Shrinkage across the face of the preheated circumferential seam was measured at 90° intervals around the seam for the N-SAW portion only. The measurements were taken with a vernier scale after each layer. Transverse shrinkage across the top of the gap is recorded in Table 9 and the average values are graphically displayed in Figure 7; values that appear anomalous (e.g. see layer 21, 270°) have been ignored in presenting this data. The results suggest three stages of joint shrinkage. Stage 1 shows an initial expansion of the weld preparation followed by a rapidly increasing shrinkage up to approximately 15 layers or 38 mm of weld deposit. Stage 2 shows a declining and then zero shrinkage from approximately 15 layers to 43 layers or 95 mm of weld deposit. Stage 3 shows a further increase in shrinkage leading to a constant value of 1.75 mm. Shrinkage across the gauge marks located 38 mm either side of the weld seam are recorded in Table 10 and shown graphically in Figure 7; shrinkage values after layers 3 to 13 at the 270° reference point are extremely high compared to those at the remaining reference points and these apparent anomalies have been ignored in presenting the data in Figure 7. In general, the shrinkage across the gauge marks followed the three zones described above; the final shrinkage value was 1.5 mm.

4.2 Nondestructive Examination Results

Magnetic particle examination of the longitudinal seam after welding and surface conditioning showed no indications at the face of the weld. Two transverse cracks were noted at the weld root, the location of these was coincident with partial penetration butt welds in the backing bar. The transverse indications were 50 and 25 mm long and had propagated from the weld metal into the base plate. Ultrasonic examination established the depth as 54 and 32 mm deep respectively (see Figure 8). The balance of the 1.83 m longitudinal seam was acceptable to the ASME B&PV Code Section VIII Division 2 magnetic particle examination criteria. Radiographic examination prior to PWHT showed the longitudinal seam to be sound away from the root cracks. Standard ASME Code and tandem probe ultrasonic examination showed the seam to be acceptable, away from the cracks, to ASME B&PV Code, Section VIII, Div. 2 requirements.

The smaller of the two root cracks was removed by carbon-arc gouging followed by grinding to a radiused contour to avoid further cracking during Q&T. The cavity was examined by magnetic particle inspection and

was not weld repaired. The shell section was flame cut through the larger defect to produce the two sections later to be joined by circumferential seam welding. After final PWHT the longitudinal seam was again subjected to ultrasonic inspection. Only one small and acceptable slag indication was detected by normal beam examination.

Radiographic and magnetic particle examination of the circumferential seam after welding and after final PWHT showed the weld to be acceptable to ASME B&PV Code, Section VIII, Div. 2 requirements. Single probe ultrasonic examination showed a line of slag at one side wall at the root of the conventional weld used to complete the outside surface. This unacceptable indication (125 percent DAC, 55 mm long) is attributed to an area of undercut which had not been removed by machining out the top of the N-SAW weld metal prior to completion of the seam with conventional SAW. The tandem probe technique revealed two lack of fusion defects at the same side wall of the narrow gap weld. A 30 mm long indication (65 percent DAC) was located at mid-thickness and a 160 mm long indication (80% DAC) was located approximately 12 mm above the root of the weld. The incidence of these defects is attributed to the guidance system problems described in paragraph 3.4. Tandem probe inspection also revealed about 20 isolated and short reflectors at the fusion boundary each producing less than 20 percent DAC. One of these defects was located for removal with the test sample for identification.

A repeat ultrasonic examination of the circumferential seam after final PWHT showed no further unacceptable indications but an increase in the number of reportable indications. Prior to PWHT, straight beam examination revealed five reportable slag indications, three of which were found after PWHT. Eight new, reportable slag indications were located after PWHT, all well below the reject level (viz. 25% to 65% of the reference amplitude). Shear wave examination prior to PWHT had shown one rejectable slag inclusion at the root of the outside weld; after PWHT, six new, reportable slag indications were located. All indications were well below the reject level (viz. 20% to 50% of the reference amplitude). Tandem probe UT examination prior to PWHT had revealed two rejectable lack of fusion defects in the N-SAW weld metal. After PWHT, three new, reportable indications were located within the N-SAW weld metal. Two of these new indications were identified as slag, one being lack of fusion but all three were well below the reject levels (viz. 25% to 30% of the reference amplitude). The appearance of new, reportable indications at low amplitude levels after PWHT is not considered significant, moreover they reflect upon the variability of the UT examination process.

4.3 Weld Metal Composition

The composition of the circumferential seam weld metal is given in Table 11 together with the analysis of the welding wire. The Carbon content

(0.084 percent) is considered low and only marginally improved over that (0.072 percent) obtained with the conventional UV420TTR flux (4). Repeat analyses by an independent laboratory were performed on samples removed from the initial test location and gave a result of 0.08 percent Carbon. Analysis for Carbon at the T/2 location gave the following results as a function of groove location: W/2, 0.079 percent; W/4, 0.081 percent.

The oxygen levels reported in Table 11 are the mean values from samples taken 76 and 127 mm from the face of the weld, viz. 282/326 ppm and 276/314 ppm Oxygen respectively. These levels of Oxygen are in line with those previously noted for UV420TTR flux welded seams (4). The temper embrittlement factor, J=69, is significantly lower than the maximum value of 200 to avoid temper embrittlement (1). The sulphur level (0.004 percent) is also conducive to high temperature toughness levels (9).

4.4 Charpy V-Notch Impact Toughness

The Charpy V-Notch specimens from the circumferential N-SAW seam at the T/2 location and notched at both W/4 and W/2 locations were tested at -40°C to establish the weld gap location of minimum toughness. The results are recorded in Table 12-1. The average value at W/4 is 131J and at W/2 is 160J showing the W/4 location to be of lower toughness. Toughness data from specimens removed from the T/4 and 3T/4 depth locations, notched at the location of minimum toughness (W/4) and tested at -40°C are recorded in Table 12-2. The average value at T/4 is 176J, at T/2 is 131J and at 3T/4 is 98J showing the 3T/4 depth to be the location of lowest toughness at W/4. The range of energy values also varies with depth location, viz. 57J at T/4, 50J at T/2 and 108J at 3T/4. Note that the lowest average absorbed energy is above the 54J minimum aim value at -40°C.

Charpy V-Notch specimens were removed from the 3T/4 depth, notched at the W/4 location and tested to produce a transition curve at Tmin and Wmin; the results are recorded in Table 12-3 and plotted in Figure 9. The 54J transition temperature is -46°C and the absorbed energy at -40°C is 97J average. A trend toward lower scatter in energy values toward the lower shelf is shown in Figure 9.

Specimens removed from the circumferential seam at 1.6 mm below the ID surface (10) were notched at the gap mid-width to provide a transition curve. This area was welded with conventional SAW but used the same consumables and parameters used for narrow gap welding. The results are recorded in Table 12-4 and plotted in Figure 10. The 54J transition temperature is below -50°C and the absorbed energy at -40°C is 116J average.

The variation in toughness through the circumferential seam depth is summarized in Table 13 which clearly indicates the 3T/4 depth, W/4 test location to be of lowest toughness.

Figure 11 relates the absorbed energy for all specimens tested in this program with the corresponding percentage shear values. It indicates that the 50 percent Fracture Appearance Transition Temperature (FATT) corresponds to 108J average with a 54J minimum.

4.5 Weld Metal Structure

The macrostructure of the N-SAW weld consists of three distinct regions (Figure 12). The most predominant region is occupied by the coarse, columnar grains of as-deposited metal which typically at the W/4 location is 0.5 to 0.7 mm deep. These regions are separated by a band of recrystalised weld metal which typically at the W/4 location is 0.1 to 0.3 mm deep. The third region, located at W/2, is a zig-zag region of recrystalised weld metal varying in width from 1.3 to 2.5 mm. The grain size within each of these three zones is characterized in Figures 13, 14 and 15 which confirms that the central (W/2) region is consistently of finer austenite grain size. The microstructure in all regions shows a bainitic transformation product but differences in bainite substructure could not be resolved by optical metallography.

The cross-section removed from the circumferential seam to identify the small ultrasonic indications noted in para. 4.2 was ground at 1.6 mm intervals with intermediate magnetic particle examinations but no defect in the surfaces so exposed could be located.

The following Charpy specimens were examined at the fracture face by Scanning Electron Microscopy; these specimens showed extremes when tested at the same temperature from two locations:

Specimen No.	Location	Absorbed Energy
73	3T/4, W/4	27J
83	3T/4, W/4	135J
125	1.6 mm, W/2	60J
105	1.6 mm, W/2	168J

Specimen No. 83 showed an area of ductile tearing at the fracture face opposite the notch, a mixture of intergranular fracture and cleavage in the centre of the specimen and 70 percent intergranular fracture at the notch (Figure 16).

Specimen No. 73 showed ductile bands at the edge opposite the notch (Figure 17), largely cleavage zones in the centre of the fracture face and again increasing proportions of intergranular fracture toward the notch to a maximum of 30%. The cleavage facets were very small, in the order of 10 x 10 μm.

The fracture face of Specimen 105 was typical of ductile fracture but again with a significant quantity (20 percent) of intergranular fracture (Figure 18). Specimen 125 exhibited largely intergranular and cleavage bands (Figure 19).

Typical microhardness surveys across the circumferential seam are summarized in Figures 20 to 23 for the four locations that were impact tested. Repeat surveys at the same location did not reproduce the apparent peak values within the refined weld metal; surveys of the columnar and refined regions showed no significant difference in hardness within the regions, viz. 205 to 230 BHN, average value 215 BHN. Local hardness values exceed the 225 BHN maximum frequently specified for petrochemical service.

5.0 DISCUSSION

Forming and welding of the experimental shell has revealed several factors which are significant to the fabrication of heavy wall pressure vessels using 2¼Cr-1Mo plate.

The 9.2 mm loss of wall thickness resulting from thermal processing of the plate is significantly greater than the 3 mm expected during plate forming C-Mn steel. The 8 mm loss in thickness after hot forming is attributed to the higher temperature to which the plate was heated (995°C compared to 900°C used for heating C-Mn steel). Additionally, the furnace used to initially heat the flat plate and that used to heat the partially formed shell were both oil fired and operated with an excess air to oil ratio. The excess air would have exaggerated surface oxidation and a reducing atmosphere or gas fired furnaces would significantly limit scaling. A further loss of 1.2 mm in thickness was recorded after Q&T and subsequent shot blasting; this value also includes oxidation losses that occurred during the final PWHT of the circumferential seam. Heating prior to quenching involved a 5 h soak at 940°C so that the reduced loss in thickness during Q&T reflects the benefit of using gas fired furnaces.

The length of flare out at the edges of the shell resulting from forming is much greater than for C-Mn steel. This may be related to forming the 2¼Cr-1Mo plate at higher temperatures which allows more flow. The magnitude of the flare out has a significant impact on material costs either if the width of discard from the edges is increased or if the plate is ordered thicker to compensate for the thinning associated with the flare out.

Generally the 1.83 m longitudinal seam welded with a tandem Arc AC-AC weld procedure was examined and found to comply with ASME B&PV Code, Section VIII, Div. 2 requirements. The incidence of cracking of the weld

root is not a common fabrication occurrence because it is standard practice to use either one piece backing bars for longitudinal seam welding of C-Mn shells or to use full penetration butt welds in the backing bar prior to fitting the bar to the shell inside surface. However, the full length 2¼Cr-1Mo bar could not be bent to the inverted V contour used to seal the root gap so three short sections were used and the butt welds made after the backing bar was welded to the shell. The incidence of root cracking shows that 2¼Cr-1Mo weld metal is very sensitive to cracking and that normal practice of using full penetration butt welds in backing bars is mandatory for welding this material.

The second stage heating cycle for hot forming heavy section C-Mn steel plate is selected as the normalize cycle required by SA516 Gr.70 to develop material properties. For 2¼Cr-1Mo heavy section plate (>125 mm) properties cannot be developed at T/2 by air cooling so that a third heat treatment (Q&T) is required. Facilities to Q&T the experimental shell sections were not located in Ontario and a significant capital investment is necessary to provide facilities for Q&T of a reactor vessel shell section. This problem exists whether the longitudinal seam would be welded before or after QT and obviously points to one advantage of using forged shell sections from offshore.

Welding of the circumferential seam using the Esab N-SAW system was virtually problem free. The flux feed and recovery components operated satisfactorily although on several occasions the feed pressure was set too high resulting in feed hose ruptures. The control panel and the guidance system were rated highly by the operators. Mechanical removal of the slag was unnecessary with the parameters used, the slag was self-peeling to reveal beads with good operator appeal.

The main shortcoming of the system is the absence of guidance over the final 25 mm of weld gap which leaves bead location to be operator controlled. Bead placement was found difficult to control manually because of the oscillating motion of the circumferential seam and because the shallow beads deposited with the parameters used made the wire to wall distance critical to avoid side wall defects. An optional axial drift indicator from the Esab EHD system monitors movement of the shell during rotation by monitoring the weld preparation at the shell edge not being welded. The motions described above which resulted from an unusual mismatch in ovality of two shells would then be relayed to the horizontal slides causing the welding head location to move with the gap.

Approximately 6.4 m of 143 mm thick circumferential seam was welded with N-SAW and showed no unacceptable indications by radiographic or ultrasonic examinations to ASME B&PV Code, Section VIII, Div. 2 and only two unacceptable indications by tandem probe ultrasonic examination. These results are significant for the first time a circumferential seam has been welded in a production environment by N-SAW at Babcock & Wilcox Canada, especially when consideration is given to gap shrinkage not

occurring to the degree expected, the weld preparation being too wide and the attendant difficulties with setting up the N-SAW head position.

The initial expansion of the weld preparation (Stage 1 in Figure 7) during welding is attributed to an increase in joint temperature as the first beads were deposited. The subsequent rapid increase in shrinkage is equated to the ease of side wall movement in the joint restrained only by tack welds at the inside surface. It is assumed that the sinking of the weld preparation would have been a maximum at this stage. The declining and then zero rate of joint contraction is associated with an increasing depth of weld metal which provides an increasing stiffness to the joint. The third stage of shrinkage which shows further increases followed by a constant value of 1.65 mm is coincident with the change from two to three beads per layer. The additional weld bead deposited along the centre of the weld preparation will increase weld metal shrinkage stresses per unit surface area until sufficient weld metal ligament exists to withstand joint movement.

The circumferential seam side walls did not close in to the degree predicted (1½ to 2°) by welding flat test plates with backing bars (4) or by welding heavy section circumferential seams (2.2°) on backing bars (11). Consequently the maximum height to which the two layer N-SAW process could be used was 95 mm at which the gap shrinkage was constant at 1.25 mm and the original gap width was 23.8 mm. The implication from this work is that with the manufacturing method used, i.e. to weld the inside of the seam before the outside, the maximum gap width would be 24 mm which equates to a 0.8° side wall if the root is 19 mm. Obviously the manufacturing sequence is significant, if the inside seam is initially welded to provide more restraint the outside weld preparation would need re-evaluation. Monitoring a narrow gap weld from the outside on a nominal 16 mm backing is recommended to quantify the appropriate gap width.

Machining of a 0.8° side wall on a circumferential seam weld preparation for a full size reactor vessel shell section requires heavy machining equipment, either a vertical or horizontal boring mill. Only where restricted heat input during welding is necessary would the cost of joint preparation be offset by using a narrow gap configuration.

Preconditioning of the agglomerated fluxes prior to welding both shell seams was performed to minimize weld zone cracking and may not have been necessary for flux taken directly from sealed containers. The temperature for preconditioning agglomerated fluxes is generally higher than for fused fluxes because both surface absorbed and chemically combined moisture needs to be removed. The highly refractory nature of the fluxes produces problems of uniform temperature distribution through the height of the flux in a conventional flux drying oven and one manufacturer recommends conditioning in 50 mm high trays (5). Although equipment such as the Phoenix Flux Holding Oven Type 750 HT with heating

elements spaced uniformly through the height of flux may be satisfactory (5), the Rocking Flux Oven used during this program functioned well during welding trials and welding of both seams.

The improvement in Charpy toughness distribution throughout the narrow gap weld proposed by increasing the weld metal Carbon level to 0.10 percent has not been proven since Carbon levels have not be significantly increased over those previously obtained (4). This observation is significant in view of the high Carbon content of the wire used (0.12 percent C) and since the UV420TTRC flux was selected to minimize Carbon losses. Information from the flux manufacturer (8) indicates that Carbon losses are highest with SAW for wire chemistries above 0.10 percent Carbon and that welds made with UV420TTRC normally yield 0.08 to 0.09 percent Carbon.

Charpy V-Notch toughness at T/2 tested at -40°C gave an average value of 131J at W/4 and 160J at W/2. Previous tests showed the W/4 location to be of higher toughness, viz. 122J compared to 49J at W/2 (4). Information from the consumable supplier also indicates that the bead mid width (W/4 in this test weld) shows higher toughness (8). The degree of bead overlap in this weld did not differ significantly from that noted in the full thickness weld previously studied (4). The improvement in toughness at the W/2 location may be the result of increased Carbon content. Certainly the difference in absorbed energy between the two locations has been significantly reduced and the range of energy values (difference between maximum and minimum values at any test location) is notably reduced from that previously seen (4), viz. 50J vs 75J at W/4 and 45J vs 65J at W/2. The gap location of minimum toughness has been shown to be 3T/4 and W/4 but the average toughness values at this location exceed the 54J minimum aim value at -40°C.

On a macroscopic scale, the higher toughness exhibited at W/2 appears to be related to a finer prior austenite grain size. Scatter in values may be the result of the 10 mm Charpy notch sampling varying amounts of the coarse and fine macrostructures.

Metallographic examination has not resolved the bainite structure so that the influence of these variables cannot be considered. Although no attempt has been made to relate absorbed energy with inclusion size or distribution, in all sections examined very few inclusions were noted. Both Oxygen and Sulphur levels were low to give a value for (O + S) = 0.046 percent (9).

Attempts at rationalizing the variation in absorbed energy within the gap by examining fracture faces of broken Charpy specimens has been unsuccessful because of the presence of intergranular fracture. This feature is surprising since the level of impurity elements, especially Phosphorous and Tin were analyzed at very low levels. The variation in hardness within the weld zones is considered significant and suggests that a higher tempering temperature during final PWHT or a longer time might equalize both the hardness and toughness values.

6.0 CONCLUSIONS

1. Hot forming of 2¼Cr-1Mo plate for pressure vessels produces greater oxidation losses than for C-Mn steel and furnace atmosphere control is significant to minimizing the loss of thickness. The extent of flare out of the plate at the shell edges is almost double that encountered in hot forming C-Mn plate and a trimming allowance of one plate thickness at each edge is required to remove the thinned material.

2. The use of full penetration welds in backing bars to weld 2¼Cr-1Mo seams is mandatory to avoid transverse cracking.

3. The absence of heat treatment facilities to Q&T reactor vessel shell sections in Ontario represents a serious setback to the manufacture of such vessels.

4. The use of the Esab N-SAW system to produce sound welds in 203 mm thick 2¼Cr-1Mo plate has been proven reliable and effective provided the weld gap and angle are selected for the joint design being used. The amount of joint shrinkage also depends to a significant degree upon the manufacturing sequence selected.

5. Consideration needs to be given to temperature uniformity during conditioning of agglomerated fluxes and one oven has been shown to be effective in avoiding hydrogen cracking problems.

6. Charpy V-Notch toughness at the weld mid thickness exceeds the 54J at -40°C minimum value at both mid gap and quarter gap widths. The location exhibiting the minimum toughness at the mid thickness is the quarter gap width although differences across the gap are small.

7. The gap location showing minimum toughness is 3T/4 and W/4 but the average toughness at this location exceeds the aim value of 54J at -40°C.

7.0 REFERENCES

1. Hantsch, H. et al "Submerged Arc Narrow Gap Welding of Nuclear Reactor Components". Schweissmitteilungen - English edition for the Essen Welding Fair, 1981 - v96/97, Sept. 1981, pp 25-28.

2. Chandel, R.S. et al "Some Factors Affecting the Mechanical Properties of Submerged Arc Narrow Gap Welds". PMRL 85-41 (OP-J), Aug. 1985.

3. Personal Communications, Dr. S. Dittrich, Thyssen Draht AG, Hamm, West Germany.

4. Wright, B., "Weld Process Development for Fabrication of Heavy Wall Pressure Vessels, Part 2". DSS Contract OSQ-82-00145.

5. Personal Communication, Mr. M. Hayes, Oerlikon Industries Ltd., Houston, Texas, USA. March 1986.

6. de Sterke, A., "Some Aspects of Radiographic and Ultrasonic Testing of Welds in Steels with Thicknesses from 100-300 mm". Brit, J. Non Destr. Test. v9, 1967, pp 104-107.

7. ASME Boiler and Pressure Vessel Code, Section VIII, Division 2, Article F-1. 1986 Edition.

8. Personal Communication, Dr. S. Dittrich, Thyssen Draht AG, Hamm, West Germany. Oct. 1987.

9. Chandel, R.S. et al "The Mechanical Properties of 2¼Cr-1Mo Weld Metal Deposited by the SAW-NG Process", PMRL 84-52(J). August 1984.

10. ASME Boiler and Pressure Vessel Code, Section VIII, Division 2, Article T-2. 1986 Edition.

11. Personal Communication, Mr. J. Hunt, Babcock & Wilcox Co. Ltd., Barberton, Ohio, USA. July 1987.

12. Personal Communication, Dr. H. Kerr, University of Waterloo, January 1988

TABLE 1

PROPERTIES OF 2¼CR-1MO PLATE FOR SHELL FABRICATION
(SUPPLIED BY CREUSOT MARREL, FRANCE)

CHEMICAL ANALYSIS (Percent)

Heat N°	C	Mn	Si	Cr	Mo	S	P	Cu	Ni	Sn	Sb	As	Ti	Cb	V	J[1]
86451.1	0.135	0.56	0.18	2.27	1.02	0.003	0.005	0.06	0.09	0.006	<0.002	0.008	<0.002	<0.005	<0.005	81

Note 1 $J = (Si + Mn)(P + Sn) \times 10^4$

MECHANICAL PROPERTIES (transverse orientation located at 1/4T)[2]

	TS MPa	YS MPa	El %	RA %	Cv-40°C J	
86451.1	554	399	26	66	114-128-142	Normalise 920°C Water Quench. Temper 650°C PWHT 690°C/24h.
					82-97-130	As above plus Socal Step Cool.

Note 2 Impact test properties were established at 1/2T location.

TABLE 2

LONGITUDINAL SEAM TEST PLATE

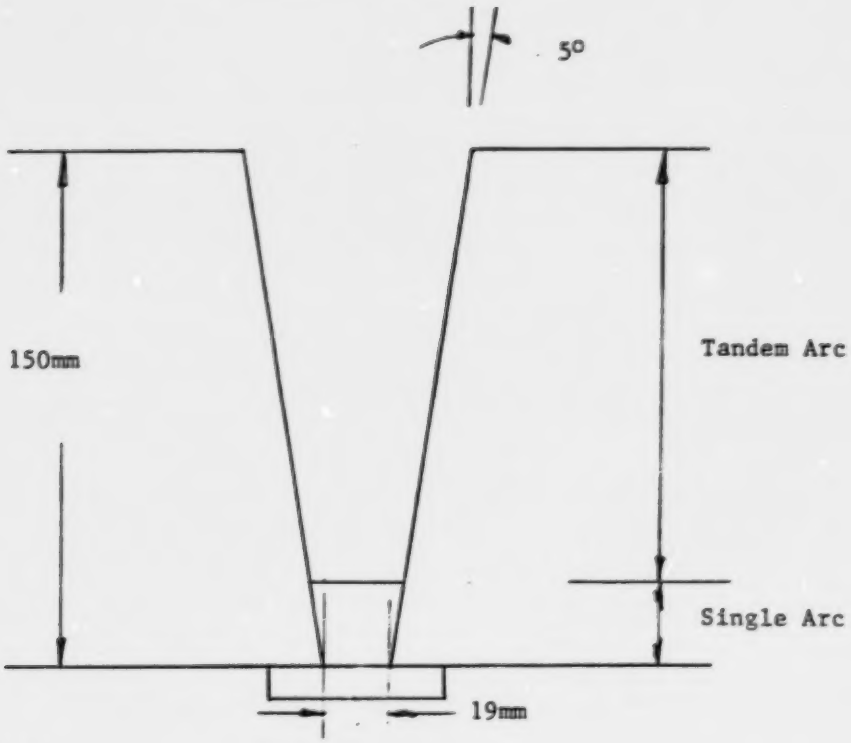

WELDING CONSUMABLES

4mm dia Oerlikon (Armco) EB3 wire, Heat No. 45324.
Chemical Analysis (percent):

0.12C	0.53Mn	0.15Si	0.009S	0.010P	2.76Cr	1.00Mo
0.22Cu	0.009Sn	<0.004Sb	0.007As			

Oerlikon OP76 Flux, Lot No. 1031. Baked 1h/290°C.

WELDING PARAMETERS

Preheat: 150°C. Interpass: 260°C

Single Arc AC:	510A	32V	380mm/min	38mm ESO
Tandem Arc AC:	500-700A	30-35V	610mm/min	35mm ESO

TABLE 3

WELD PARAMETERS FOR LONGITUDINAL SEAM

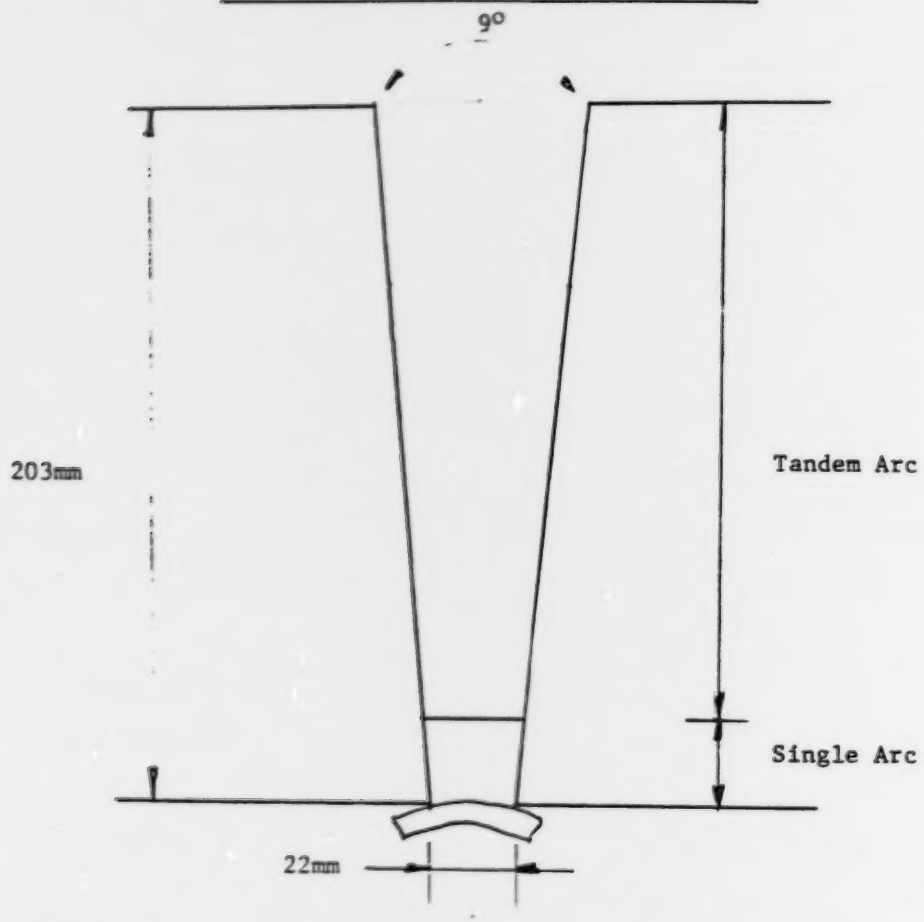

WELDING PARAMETERS

Single Arc AC:	500A	32V	380mm/min	38mm ESO
Tandem Arc AC Lead:	520-650A	30-32V	510 to 610mm/min	38mm ESO
Tandem Arc AC Trail:	550-650A	30-32V	510 to 610mm/min	38mm ESO

Preheat: 150 to 260°C

Postheat: 205 to 260°C for 4h upon completing the weld then cooled to room temperature.

TABLE 4

WELD PARAMETERS FOR NARROW GROOVE

WELDING CONSUMABLES

4mm dia Thyssen S1 CrMo2 (EB-3), Heat No. 537183

Chemical Analysis (percent):

0.12C	0.46Mn	0.10Si	0.006S	0.005P	2.62Cr	1.01Mo
0.01Cu	0.003Sn	0.002Sb	0.003As	0.02Ni	0.01V	

Thyssen UV420TTRC Flux. 8 x 48 Mesh, Lot No. 365 Baked at 350°C and held at 150°C prior to use.

WELDING PARAMETERS

Preheat: 150°C Interpass: 232°C

Single Arc, DCRP: 480-520A 32V 610mm/min 41mm ESO

(wire to wall distance 2.5 mm)

TABLE 5

PROGRAM FOR IMPACT TESTING THE CIRCUMFERENTIAL SEAM

	INITIAL PLAN	REVISED PLAN
1.	Test 5 Charpy V-Notch specimens at -40°C, located 1.6 mm below the surface, notched at quarter groove width (W/4) and half groove width (W/2) to establish the location with the minimum toughness (Wmin).	Test 5 Charpy V-Notch specimens at -40°C located at half thickness (T/2), notched at W/4 and W/2 to establish the location with the minimum toughness (W min) (see Note 1).
2.	Test 5 Charpy V-Notch specimens at -51°, -29° and -18°C located 1.6 mm below the surface and notched at Wmin to give a transition curve.	See para. 5 below.
3.	Test 5 Charpy V-Notch specimens at -40°C located at T/4, T/2, and 3T/4, and notched at Wmin. to establish the depth with minimum toughness (Tmin).	Test 5 Charpy V-Notch specimens at -40°C located at T/4 and 3T/4 and notched at Wmin to establish the depth with minimum toughness (Tmin) (Note 2).
4.	Test 5 Charpy V-Notch specimens at -51°, - 29° and -18° located at Tmin and notched at Wmin to establish a transition curve.	Test 5 Charpy V-Notch specimens at -51°, -29° and -18°C located at Tmin and notched at Wmin to establish a transition curve.
5.	-	Test 5 Charpy V-Notch specimens at -51°, -40°, -29° and -18°C located at 1.6 mm below the ID surface and notched at W/2 (Note 3).

Note 1:
The location 1.6 mm below the surface is not N-SAW and the alternative depth location, T/2, was selected to establish Wmin. The T/2 depth is significant in that petrochemical design specifications often require certification of properties at that depth.

Note 2:
At the 3/4T location, a two bead per layer N-SAW technique was used so that notch location can be precise at W/2 and W/4. At T/4, however, a 3 bead per layer technique was used so that notch location was identified after etching to be equivalent to the W/2 and W/4 macrostructures.

Note 3:
The inside weld preparation is more representative of conventional SAW than that at the outside and the Charpy specimens notched at W/2 will sample a composite of as-welded and refined structures for comparison to the W/2 and W/4 data from other locations.

TABLE 6

SHELL PLATE DIMENSIONAL CHANGES (mm)

SHELL INSIDE DIAMETER CHANGES:

	Side A	Side B
AFTER ROLLING:		
Minimum Diameter	1828.8	1830.4
Maximum Diameter	1835.2	1836.8
Difference	6.4	6.4
AFTER LONG. SEAM WELDING:		
Minimum Diameter	1828.8	1832.0
Maximum Diameter	1835.2	1836.8
Difference	6.4	4.8
AFTER QUENCH AND TEMPER:		
Minimum Diameter	1828.8	1827.2
Maximum Diameter	1830.4	1835.1
Difference	1.6	7.9

PLATE THICKNESS CHANGES:

Thickness as-received	208.5 mm
Thickness after second roll	200.5 mm
Thickness after quench & temper	199.3 mm

SHELL PLATE WIDTH CHANGES:

	ID	OD
Width as-received	1896	1892
Width after second roll	1913	1893
Difference	17	1

TABLE 6 (CONTINUED)

FLARE-OUT AT SHELL EDGES

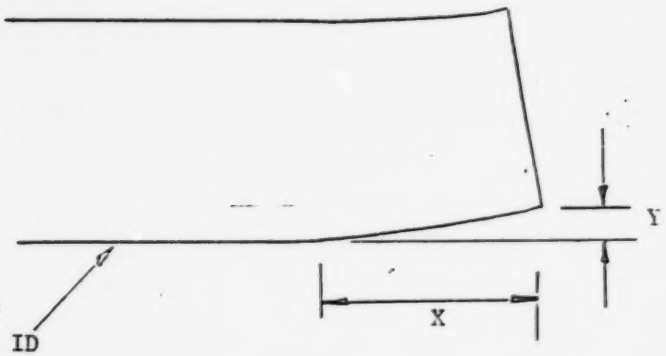

Location	Side A		Side B	
	X	Y	X	Y
1	127	5	127	5
2	165	5.5	127	5
3	203	7	152	6
4	178	6	165	6

TABLE 7

TRANSVERSE SHRINKAGE ASSOCIATED WITH CIRCUMFERENTIAL SEAM WELDING (mm)

REFERENCE	75 mm GAUGE INSIDE	610 mm GAUGE INSIDE	610 mm GAUGE OUTSIDE
PRIOR TO WELDING:			
0°	67.95	609.98	609.06
90°	67.18	609.98	610.79
180°	67.56	609.24	609.73
270°	70.74	609.98	610.49
AFTER WELDING:			
0°	67.31	609.58	609.04
90°	66.55	609.94	609.90
180°	67.72	609.04	608.51
270°	70.31	609.12	610.16
DIFFERENCE DUE TO WELDING:			
0°	-0.64	-0.40	-0.02
90°	-1.63	-0.04	-0.89
180°	+0.16	-0.20	-1.22
270°	-0.43	-0.86	-0.33
AFTER PWHT:			
0°	na	609.75	609.55
90°	na	609.75	609.98
180°	na	608.71	609.02
270°	na	608.68	608.74
DIFFERENCE DUE TO PWHT:			
0°	na	+0.17	+0.51
90°	na	-0.19	+0.08
180°	na	-0.33	-0.49
270°	na	+0.56	+1.42

TABLE 8

CHANGES IN INSIDE DIAMETER ASSOCIATED WITH CIRCUMFERENTIAL SEAM WELDING (mm)

REFERENCE	610 mm GAUGE SIDE A	50 mm GAUGE SIDE A	50 mm GAUGE SIDE B	610 mm GAUGE SIDE B
PRIOR TO WELDING:				
0°	1835.76	1833.75	1835.66	1834.49
90°	1832.25	1829.16	1831.54	1830.45
AFTER WELDING:				
0°	1835.48	1833.27	1830.55	1834.49
90°	1832.15	1828.98	1830.40	1830.25
DIFFERENCE DUE TO WELDING:				
0°	-0.28	-0.48	-5.11	0
90°	-0.10	-0.18	-1.14	-0.20
AFTER PWHT:				
0°	1835.88	na	na	1834.44
90°	1831.92	na	na	1830.55
DIFFERENCE DUE TO PWHT:				
0°	+0.40	na	na	-0.05
90°	-0.23	na	na	+0.30

TABLE 9

TRANSVERSE SHRINKAGE OF CIRCUMFERENTIAL SEAM MEASURED AT FACE OF GROOVE

DEPTH OF WELD (MM)	NUMBER OF WELD LAYERS	SHRINKAGE (mm)				AVERAGE
		0°	90°	180°	270°	
0	0	0.0	0.0	0.0	0.0	0.0
6	3	+0.1	+0.1	+0.2	+0.2	-0.15
19	6	0.0	0.0	0.0	0.0	0.0
25	10	-0.2	0.0	0.0	0.0	-0.1
31	13	-0.4	-0.2	-0.2	0.0	-0.3
38	15	-1.1	-0.6	-0.9	-0.3	-0.9
44	17	-1.1	-0.6	-1.0	-0.3	-1.0
50	19	-1.2	-0.9	-1.0	-0.3	-1.0
57	21	-1.1	-1.0	-1.0	+0.2	-1.0
65	24	-1.1	-1.0	-1.0	-0.9	-1.0
74	30	-1.5	-1.4	-1.1	-1.0	-1.2
82	33	-1.8	-1.1	-1.1	-1.0	-1.2
89	37	-2.0	-1.0	-1.1	-1.0	-1.3
95	40	-1.3	-1.2	-1.3	-1.0	-1.2
108	44	-1.3	-1.4	-1.4	-1.1	-1.3
114	49	-1.4	-1.5	-1.6	-1.3	-1.45
133	52	-1.9	-1.8	-1.9	-1.6	-1.8
139	54	-1.9	-1.8	-1.7	-1.5	-1.7
146	57	-1.9	-1.7	-1.7	-0.9	-1.7

TABLE 10

TRANVERSE SHRINKAGE OF CIRCUMFERENTIAL SEAM MEASURED AT 75 MM GAUGE LENGTH ACROSS THE SEAM

DEPTH OF WELD (MM)	NUMBER OF WELD LAYERS	SHRINKAGE (mm) 0°	90°	180°	270°	AVERAGE
0	0	0.0	0.0	0.0	0.0	0.0
6	3	0.0	-0.2	-0.1	-2.3	-0.1
19	6	+0.1	-0.3	-0.2	-1.5	-0.2
25	10	0.0	-0.3	-0.2	-1.5	-0.2
31	13	-0.2	-0.5	-0.4	-1.5	-0.4
38	15	-0.9	na	-1.3	-0.7	-0.7
44	17	-0.9	-0.3	-1.4	-0.7	-0.8
50	19	-1.1	-1.0	-1.4	-1.3	-1.2
57	21	-1.0	-1.1	-1.4	-1.6	-1.2
65	24	-1.1	-1.1	-1.4	-1.7	-1.3
74	30	-1.0	-1.5	-2.3	-1.8	-1.6
82	33	-0.8	-1.2	-2.2	-1.6	-1.4
89	37	-0.9	-1.1	-2.0	-1.5	-1.3
95	40	-1.0	-1.0	-1.2	-1.5	-1.2
108	44	-1.2	-1.3	-1.2	-1.5	-1.3
114	49	-1.2	-1.7	-1.3	-1.8	-1.5
133	52	-1.5	-1.2	-1.8	-1.6	-1.5
139	5'	-1.6	-1.2	-1.7	-1.6	-1.5
146	57	-1.7	-1.2	-1.5	-1.5	-1.5

Table 11

CHEMICAL COMPOSITION OF CIRCUMFERENTIAL SEAM (percent)

	C	Mn	Si	Cr	Mo	S	P	Sn	As	Sb	Ti	V	Cb	Ni	O	N	J[1]
Weld Metal	0.084	0.69	0.23	2.4	1.1	0.004	0.006	<0.0015	0.005	<0.001	0.002	0.003	<0.010	0.027	0.030	0.016	69
Weld Wire	0.12	0.46	0.10	2.6	1.0	0.006	0.005	<0.003	0.003	0.002	0.003	0.01	0.002	0.02	-	-	-

Note 1 $J = (Si + Mn)(P + Sn) \times 10^4$

TABLE 12

CHARPY V-NOTCH IMPACT RESULTS

SPECIMEN NUMBER	ABSORBED ENERGY J	LATERAL EXP. mm	% SHEAR
1. DEPTH LOCATION: T/2. NOTCH LOCATION: W/4 AND W/2 TEST TEMPERATURE = -40°C			
W/4 Notch Location			
102	116	1.6	45
112	122	1.6	55
122	167	2.1	65
132	na	1.8	65
142	119	1.5	50
W/2 Notch Location			
52	149	1.9	63
62	154	2.0	61
72	163	2.2	60
82	188	2.5	66
92	144	2.1	42
2. DEPTH LOCATION: T/4 AND 3T/4. NOTCH LOCATION: W/4 TEST TEMPERATURE = -40°C			
T/4 Depth			
51	152	1.7	40
61	168	1.8	60
71	209	2.0	75
81	184	2.2	65
91	171	2.0	60
3T/4 Depth			
53	65	0.6	20
63	127	1.5	40
73	27	0.2	0
83	135	1.6	45
93	130	1.4	35

TABLE 12

CHARPY V-NOTCH IMPACT RESULTS (CONTINUED)

SPECIMEN NUMBER	ABSORBED ENERGY J	LATERAL EXP. mm	% SHEAR
3. DEPTH LOCATION: 3T/4. NOTCH LOCATION: W/4			
Test at -51°C			
103	60	0.9	10
113	24	0.4	5
123	18	0.4	10
133	27	0.4	10
143	22	0.3	10
Test at -29°C			
153	38	0.7	15
163	68	1.0	40
173	135	1.8	60
183	171	2.1	70
193	116	1.5	65
Test at -18°C			
203	138	1.7	60
213	116	1.5	60
223	160	2.1	70
233	190	2.3	80
243	150	1.9	75
4. DEPTH LOCATION: 1.6 mm BELOW THE ID. NOTCH LOCATION: W/2			
Test -51°C			
5S	22	0.3	5
6S	100	1.4	25
7S	96	1.4	25
8S	27	0.4	5
9S	146	1.8	30
Test -40°C			
10S	168	1.9	70
11S	103	1.2	25
12S	60	0.6	10
13S	145	2.0	60
14S	106	1.4	35

TABLE 12

CHARPY V-NOTCH IMPACT RESULTS (CONTINUED)

	SPECIMEN NUMBER	ABSORBED ENERGY J	LATERAL EXP. mm	% SHEAR
4.	DEPTH LOCATION: 1.6 mm BELOW THE ID.		NOTCH LOCATION:	W/2 (CONTINUED)
	Test -29°C			
	15S	135	1.8	35
	16S	153	2.1	50
	17S	165	2.1	55
	18S	163	1.9	45
	19S	154	2.1	45
	Test -18°C			
	20S	165	2.2	50
	21S	168	1.9	60
	22S	182	2.3	65
	23S	163	2.0	50
	24S	179	2.2	70

TABLE 13

CHARPY V-NOTCH PROPERTIES OF CIRCUMFERENTIAL SEAM AT -40°C,J (ft.lbs.)

DEPTH	W/4	W/2
T/4	Ave.: 176 (130) R: 57 (42)	na
T/2	Ave.: 131 (97) R: 51 (37)	Ave.: 160 (118) R: 44 (33)
3T/4	Ave.: 97 (72) R: 108 (80)	na
1.6 mm from ID	na	Ave.: 116 (86) R: 108 (80)

Note: a) Ave. are averages of five values.
b) R = Range of absorbed energy.
c) Results at 1.6 mm from ID, W/2 are for conventional SAW, all other results are for N-SAW.

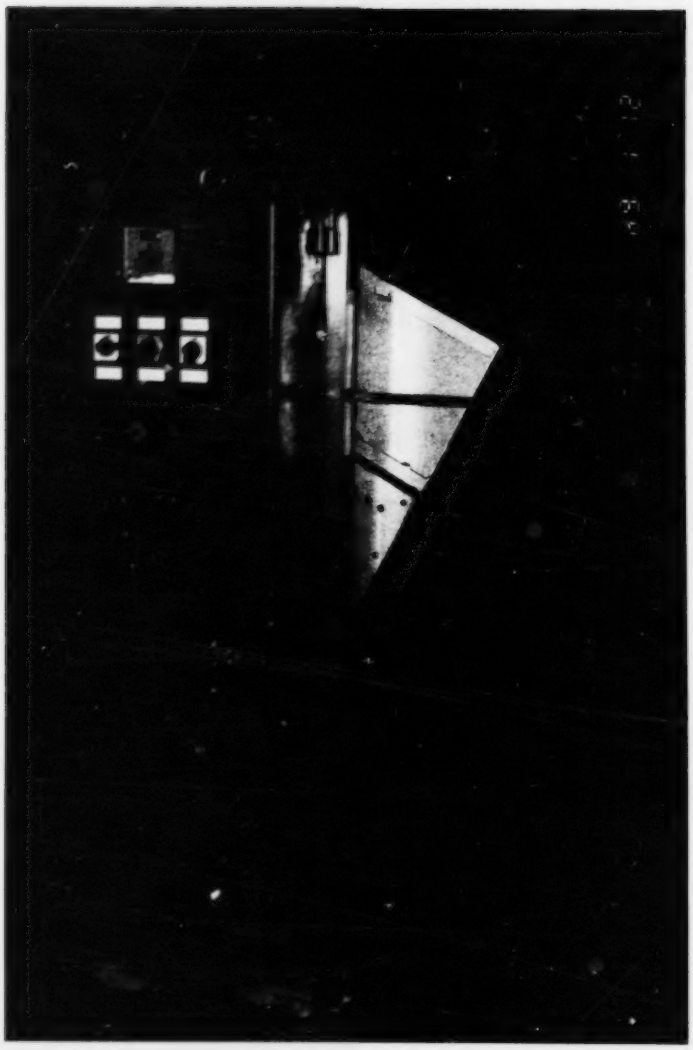

Figure 1 Flux Drying Oven UT-40A

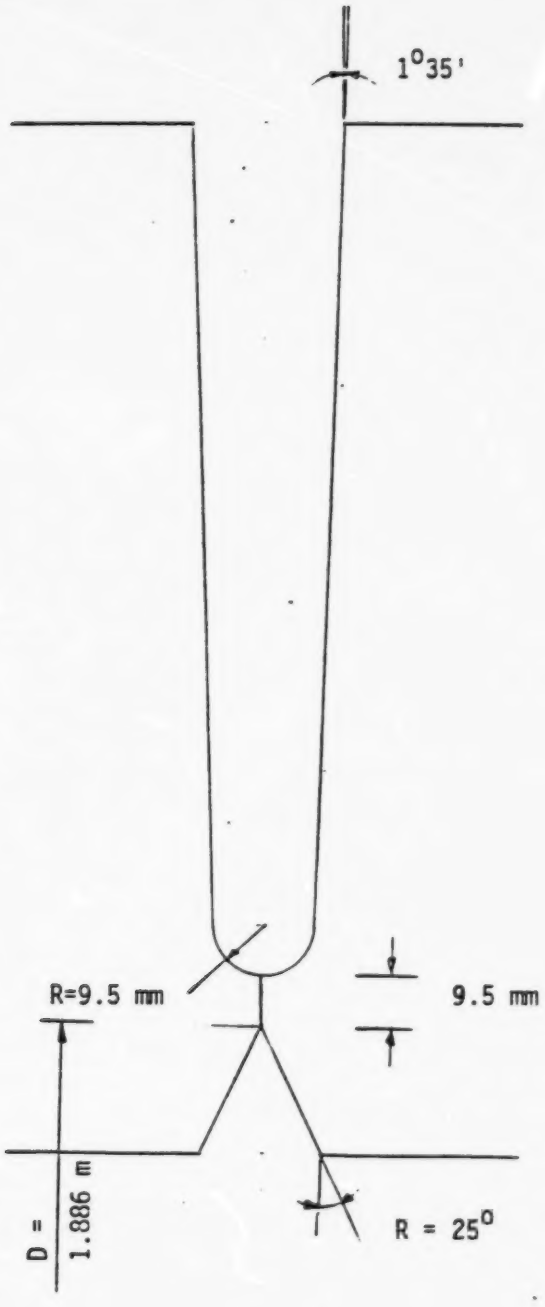

Figure 2 Detail of Circumferential Seam Weld Preparation

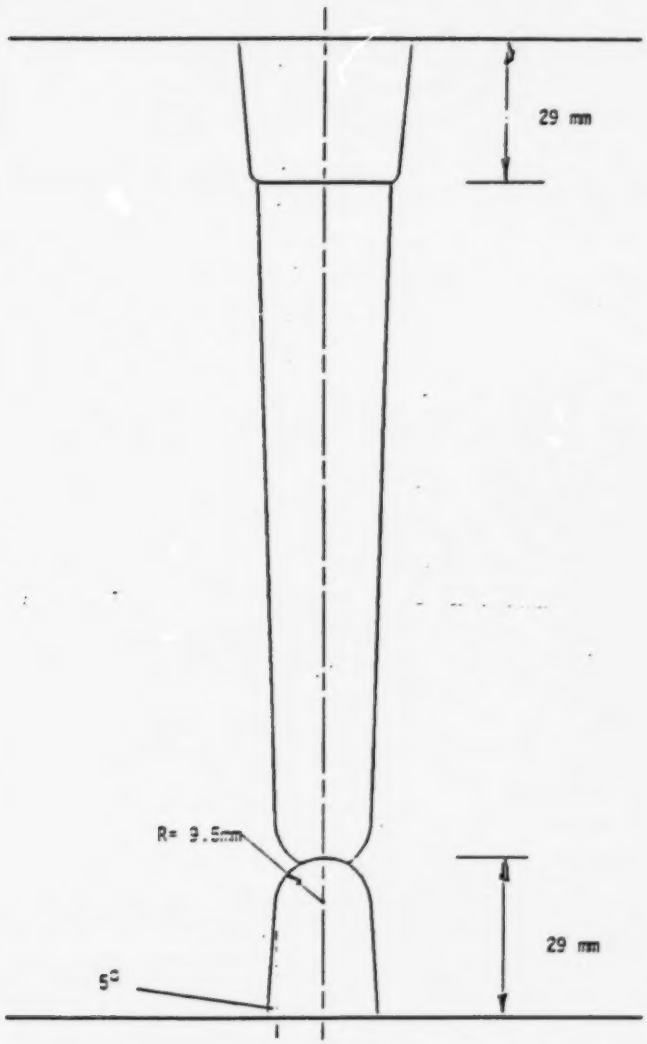

Figure 3 Final Configuration of Circumferential Seam Weld

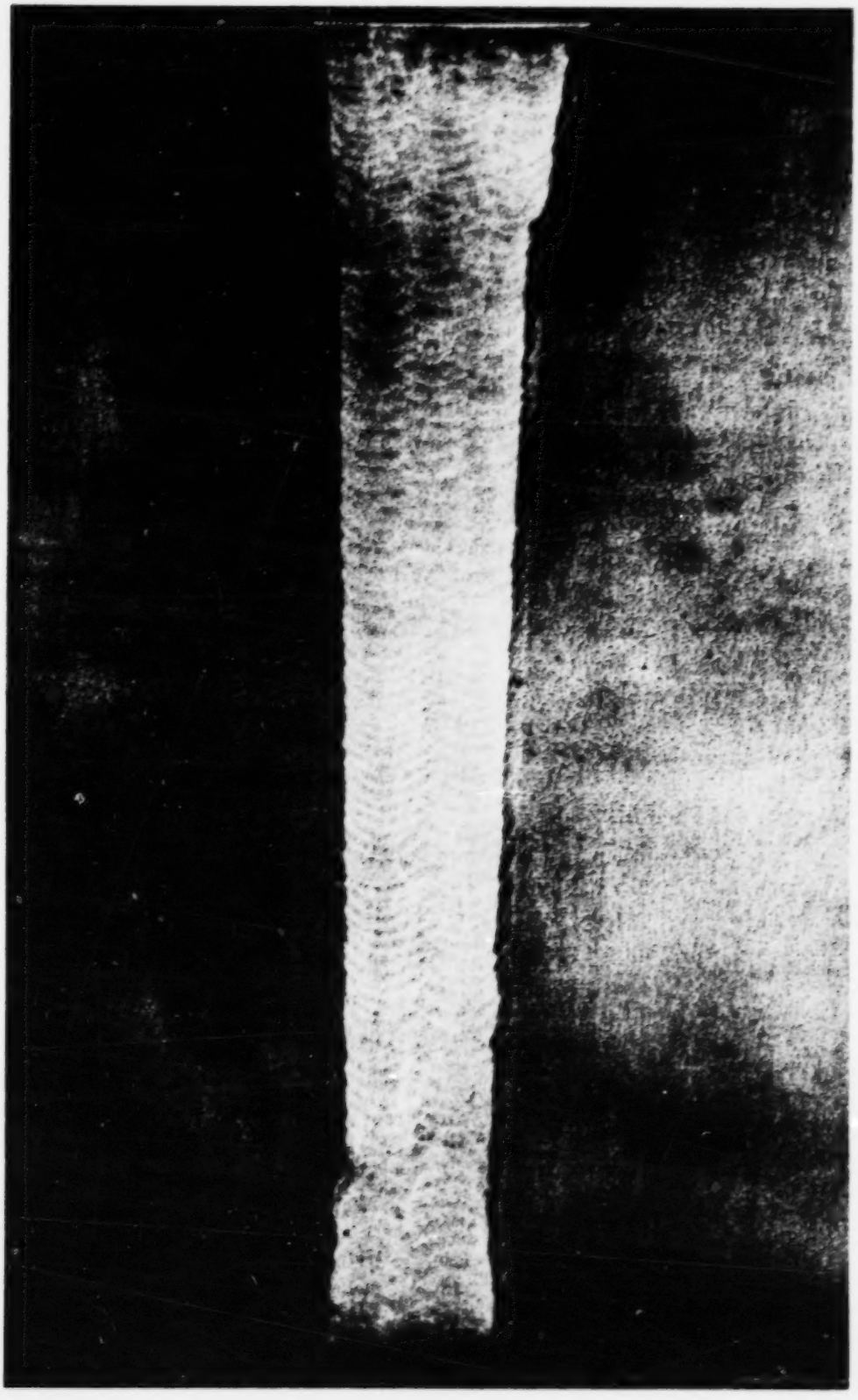

Figure 4 Macro Section of Circumferential Weld Etched in Magnification

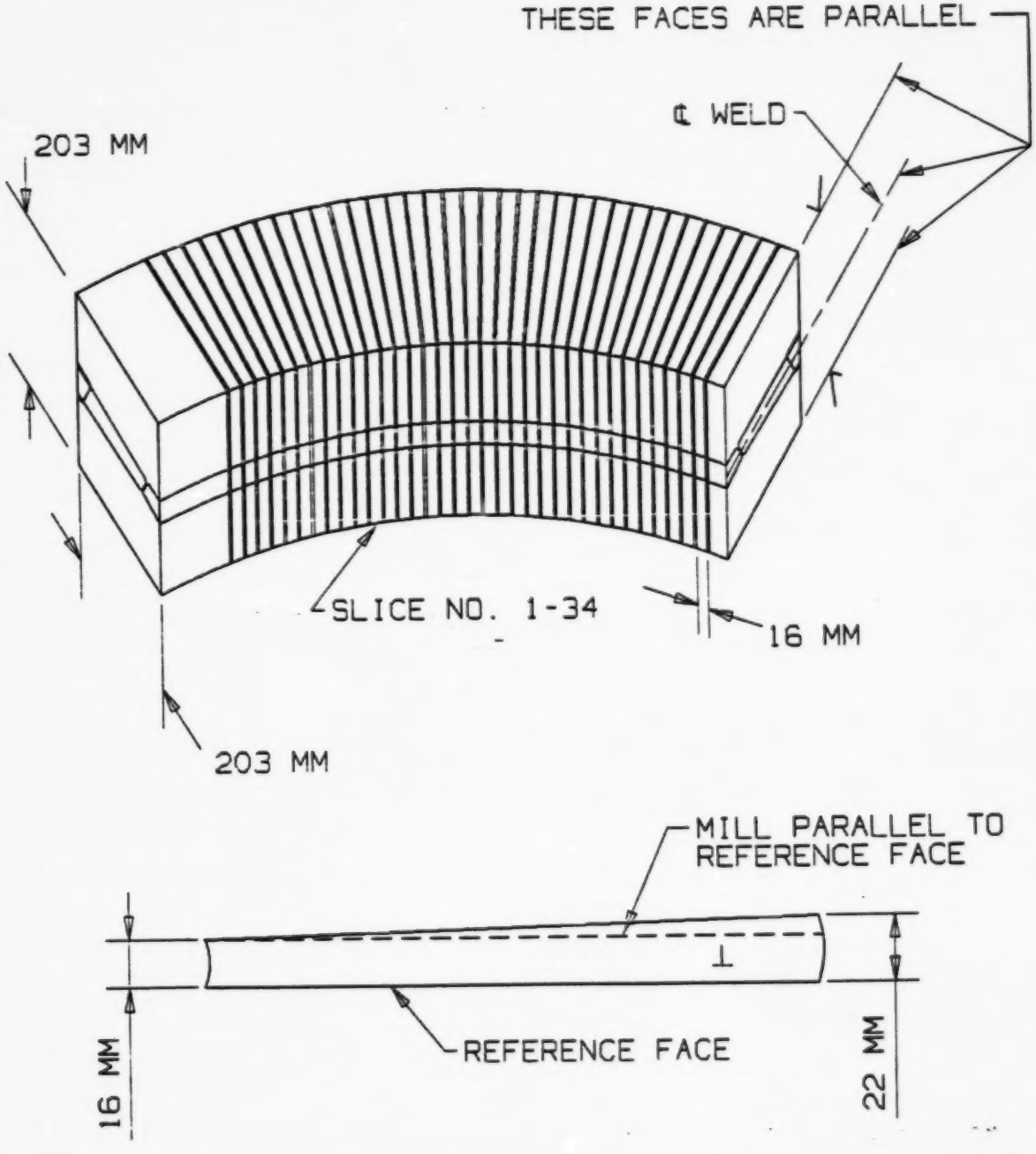

Figure 5 Test Specimen Removal from Circumferential Seam

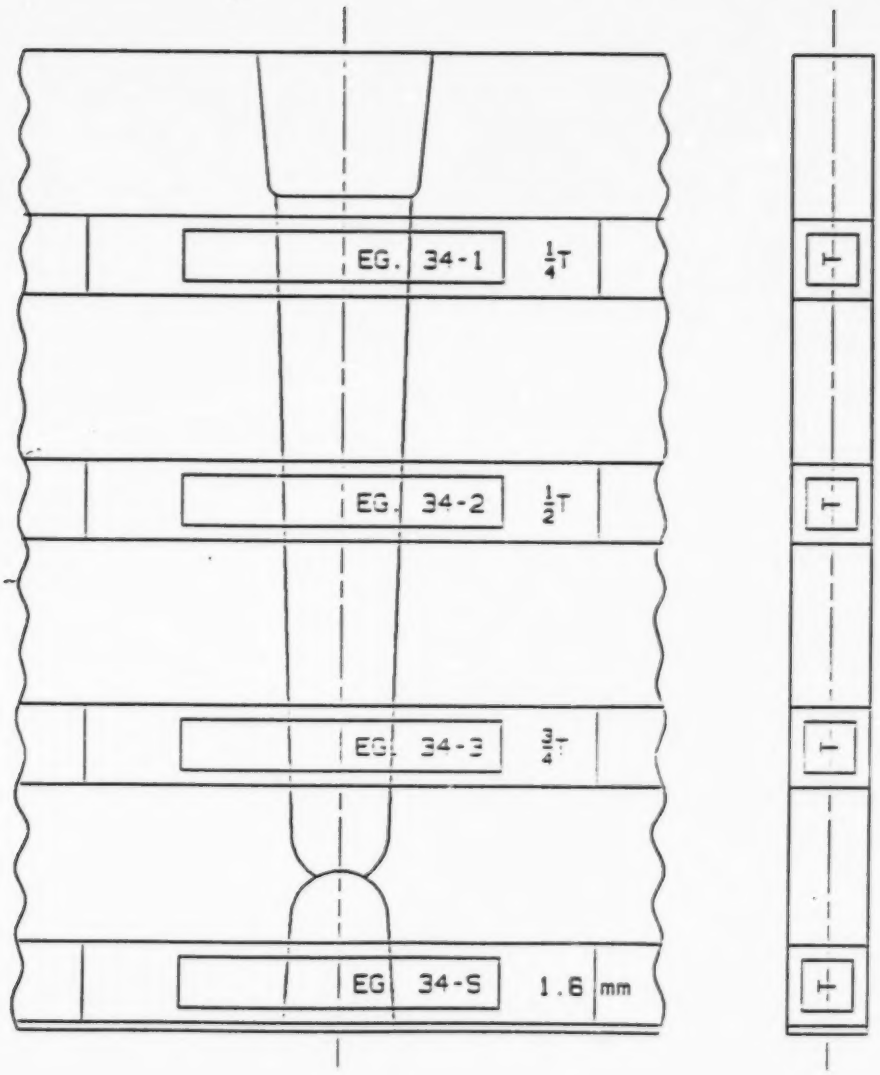

Figure 6 Charpy Test Specimen Removal

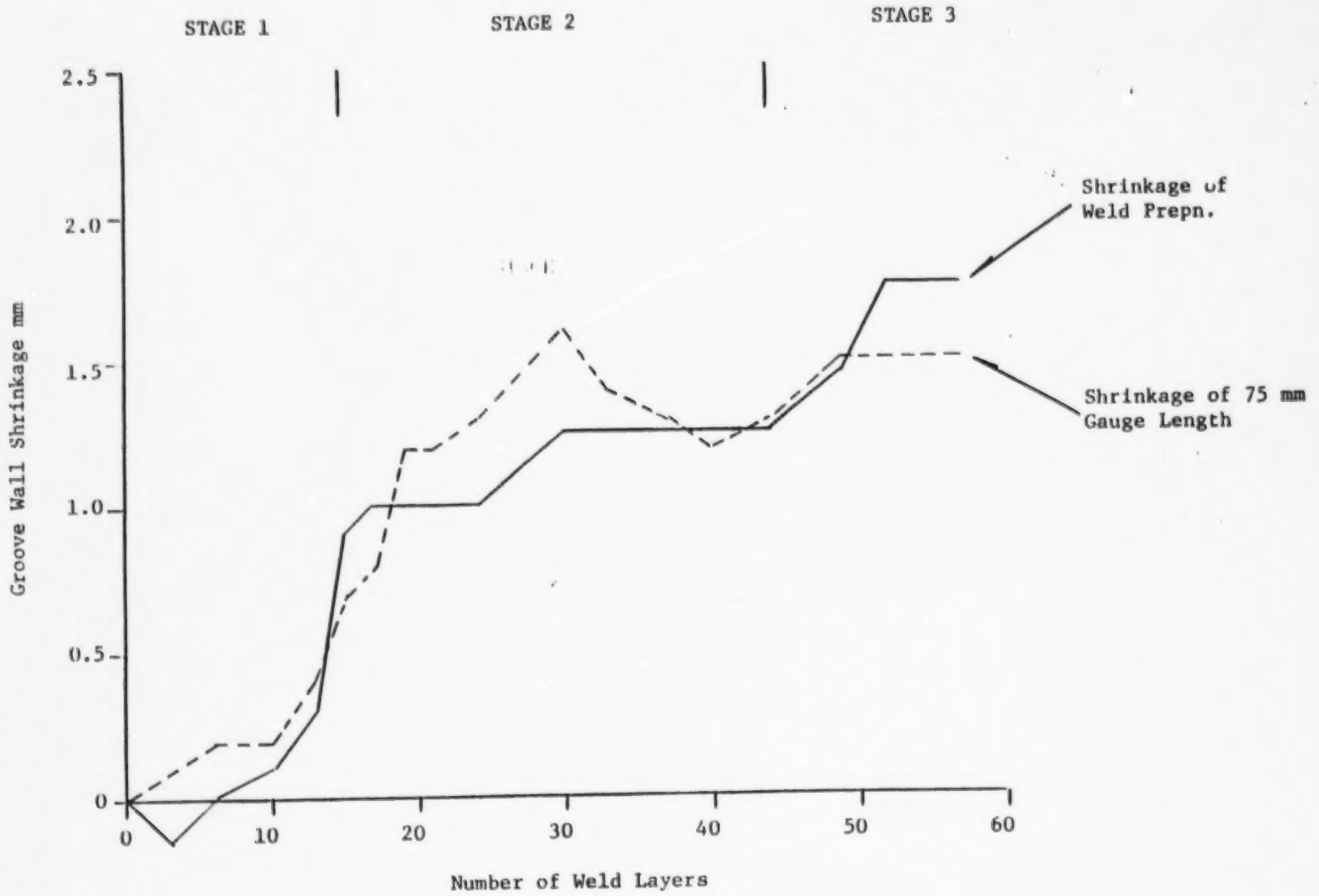

Figure 7 Transverse Shrinkage Across Circumferential Seam

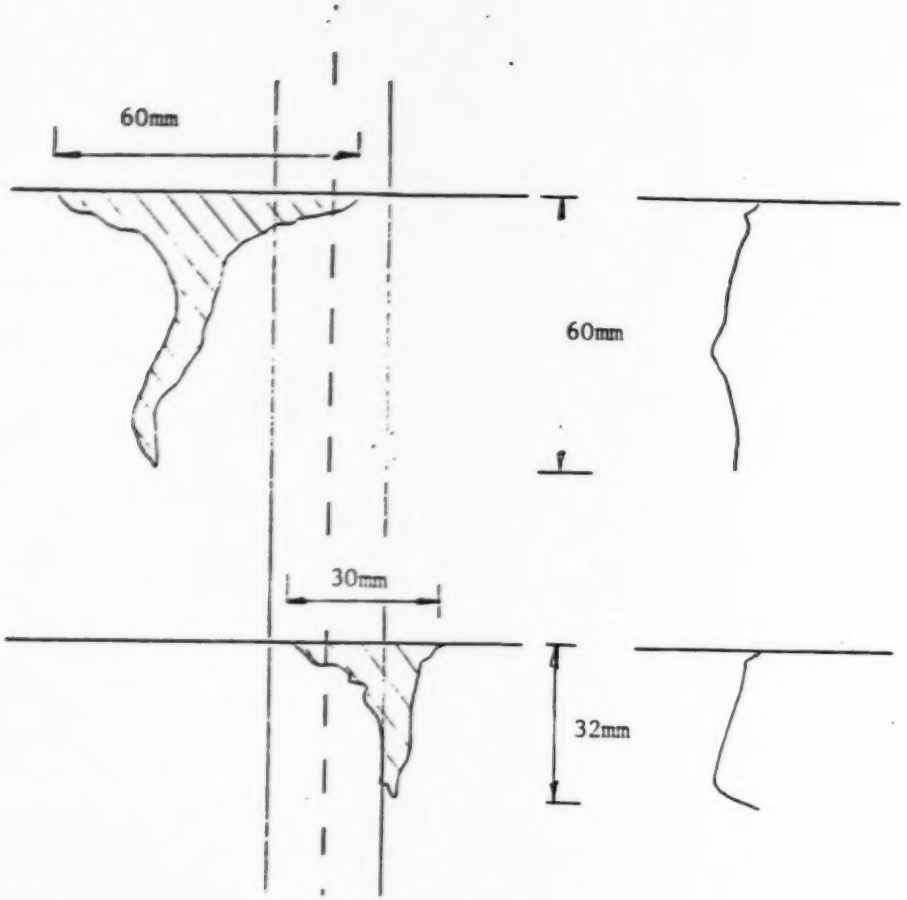

Figure 8 Contour of Longitudinal Weld Root Cracks.

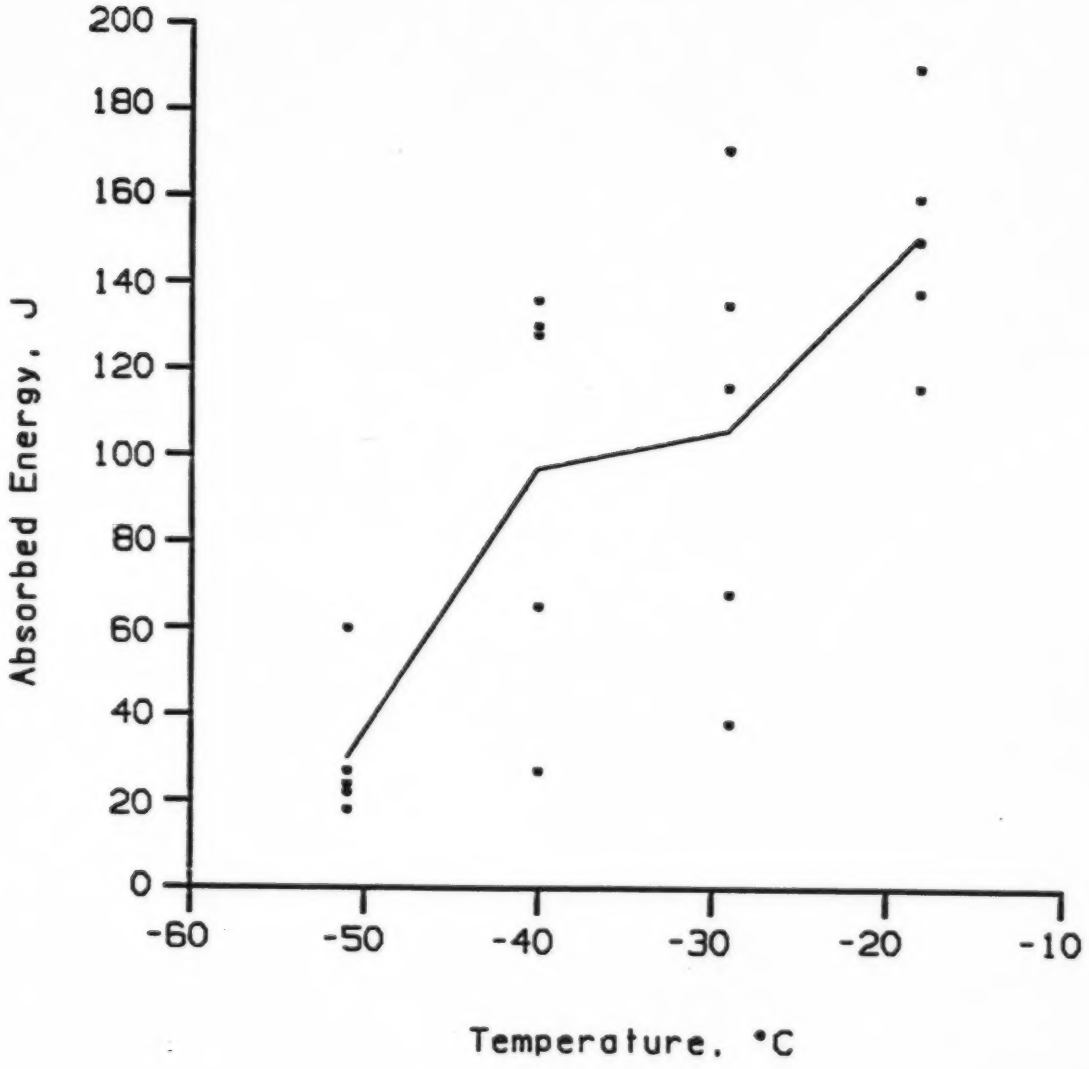

Figure 9 Charpy V-notch Transition Curve for N-SAW, 3T/4 Location Notched at 1/4W

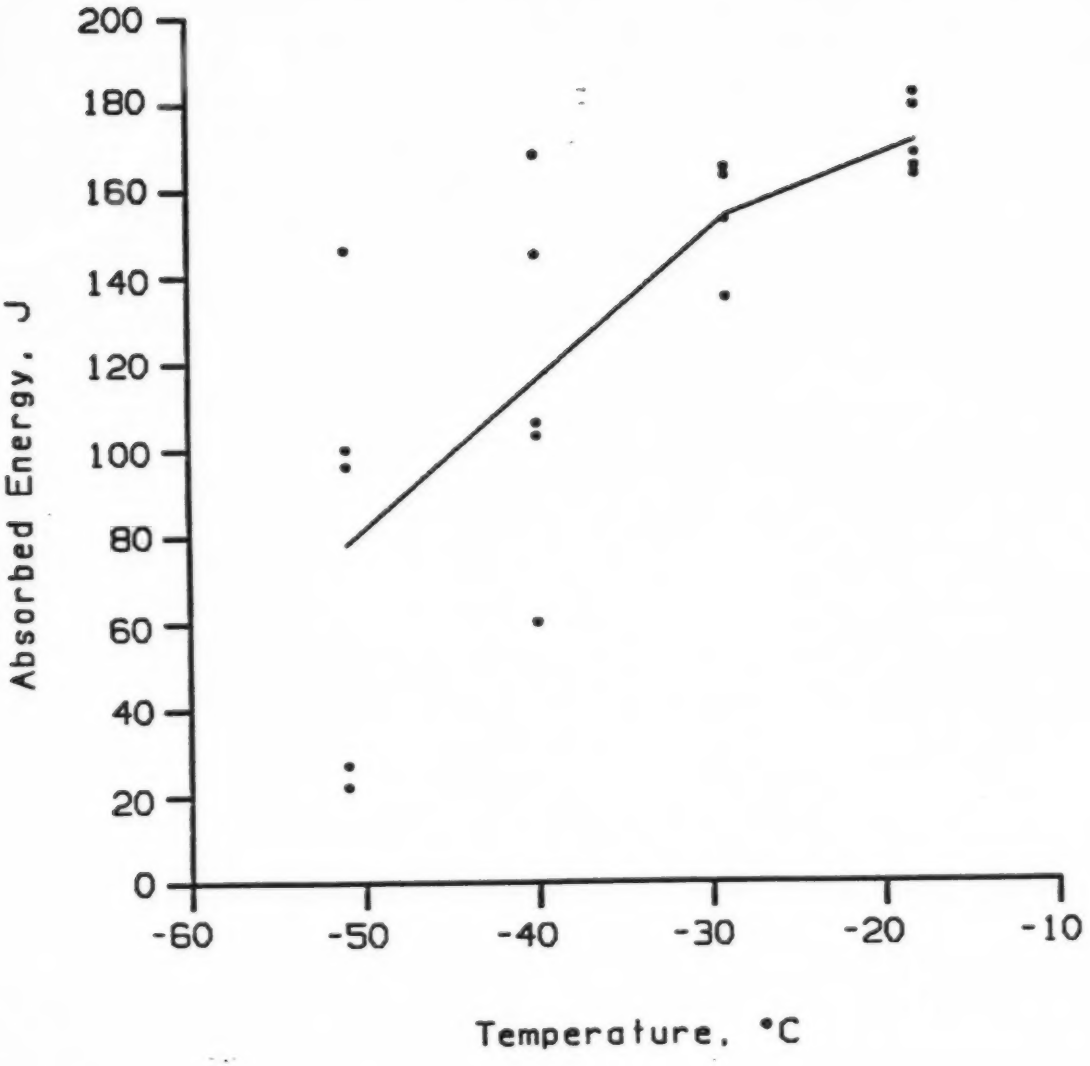

Figure 10 Charpy V-notch Transition Curve for Conventional SAW, 1.6mm Below the ID Surface, Notched at W/2.

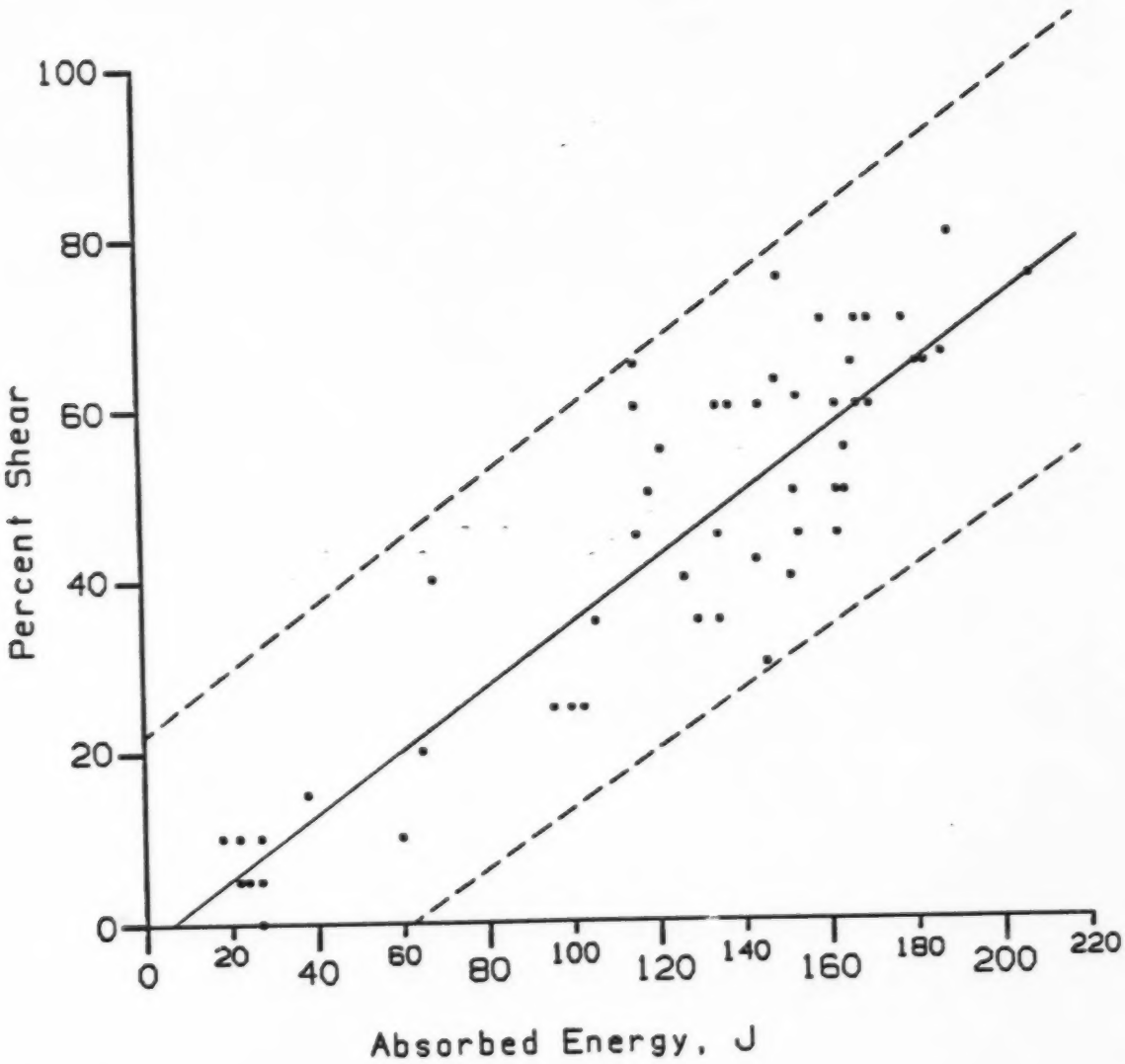

Figure 11 Relationship Between Absorbed Energy and Percent Shear for Weld Metal Charpy Specimens.

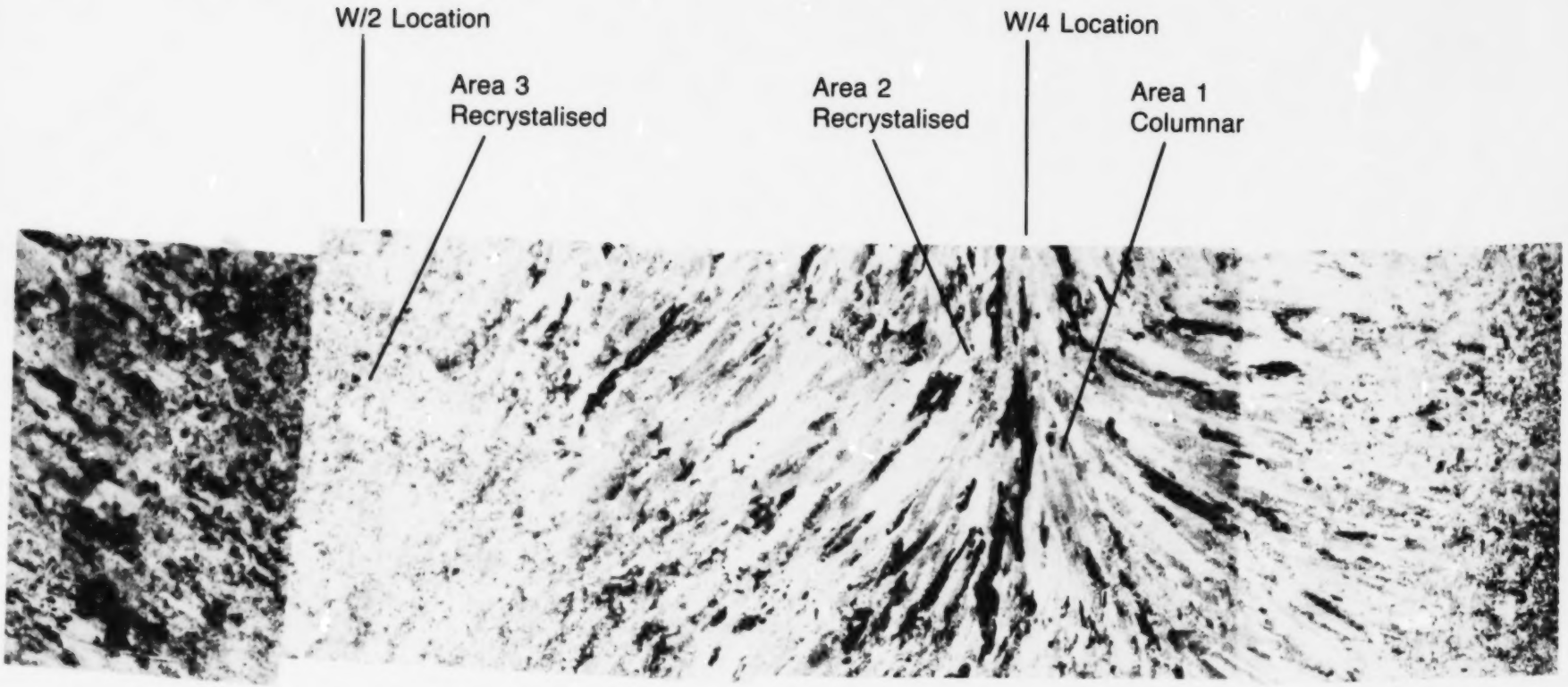

Figure 12 Typical Macrostructure of N-SAW Weld Metal
Etched: Saturated Picral. Magnification X 60

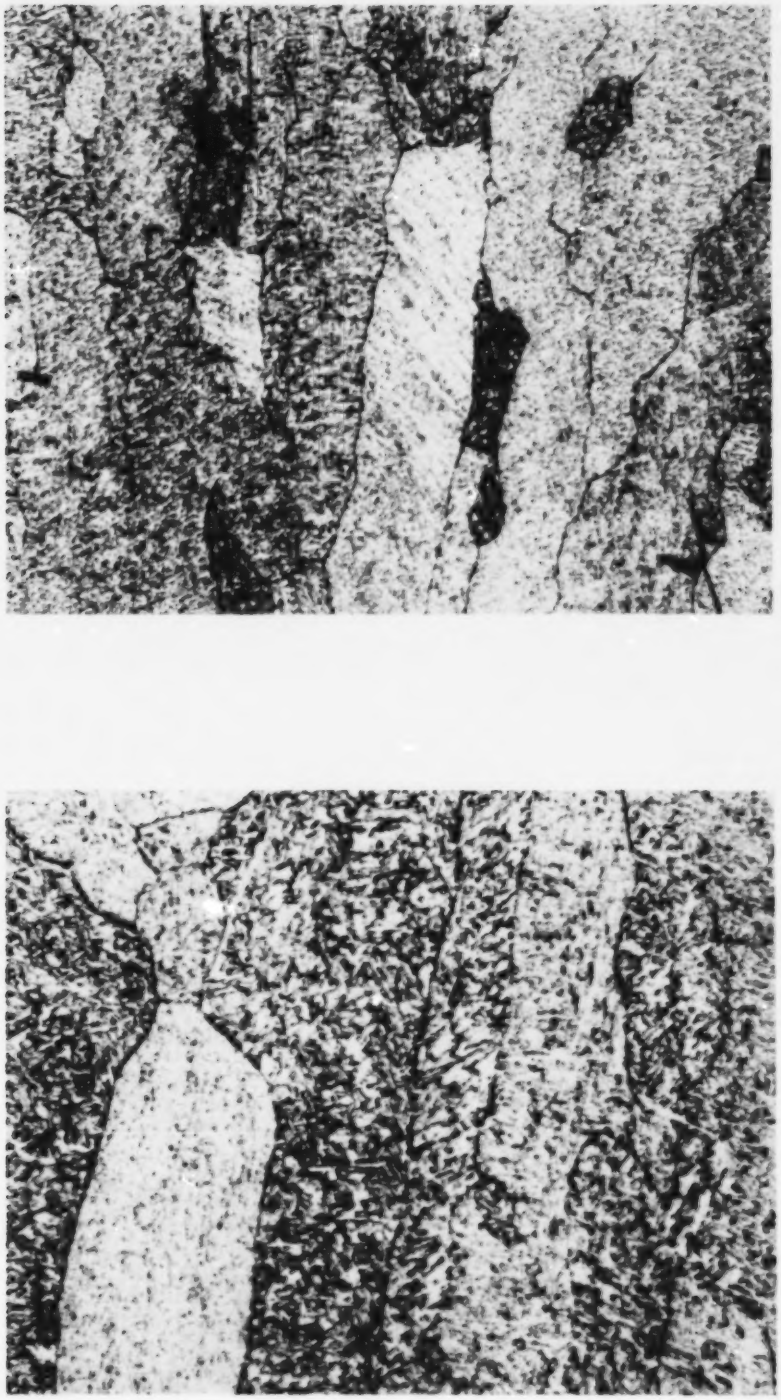

Figure 13 Bainitic Structure in Area 1, 3/4T
Etched: Saturated Picric Acid + 1% Nital
Magnification: X150 (top), X300 (bottom)

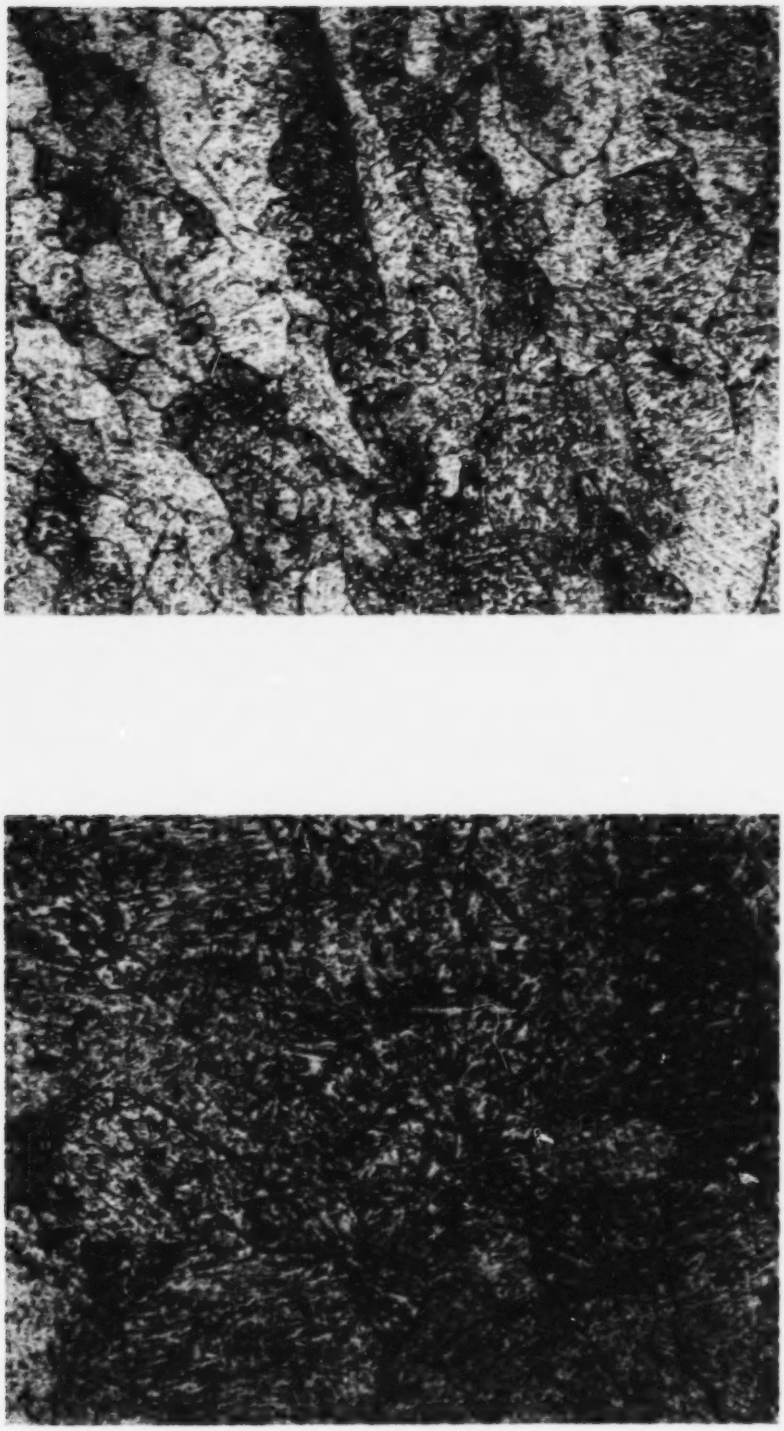

Figure 14 Bainitic Structure in Area 2, 3/4T
Etched: Saturated Picric Acid + 1% Nital
Magnification: X150 (top), X300 (bottom)

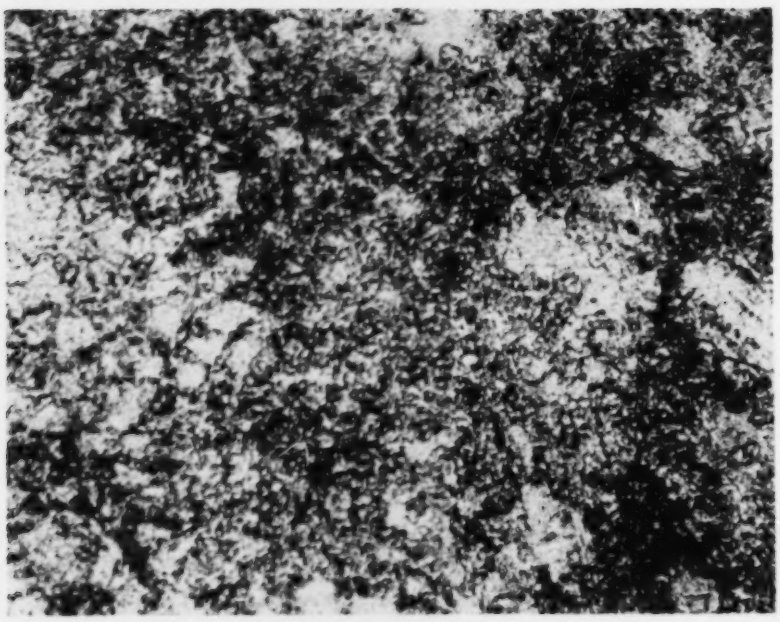

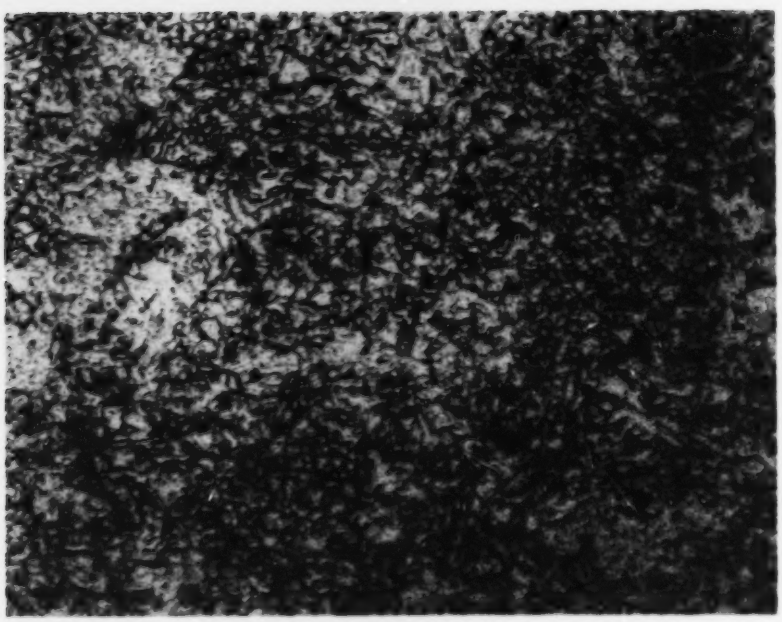

Figure 15 Bainitic Structure in Area 3, 3/4T
Etched: Saturated Picric Acid + 1% Nital
Magnification: X150 (top), X300 (bottom)

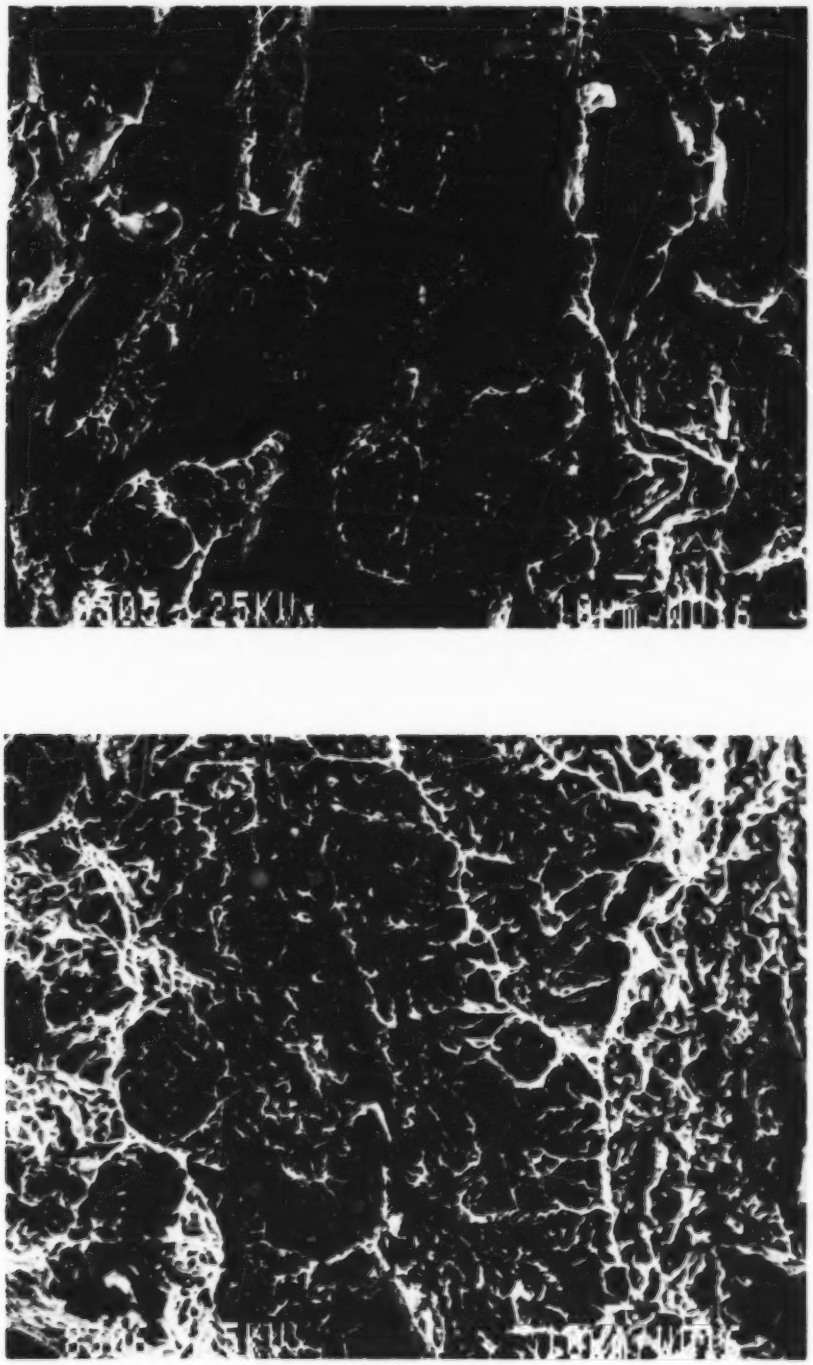

Figure 16 Fracture Appearance of Charpy Sample No. 83
Top: Toward Notch: 60% Intergranular
Bottom: Middle of Sample: Cleavage

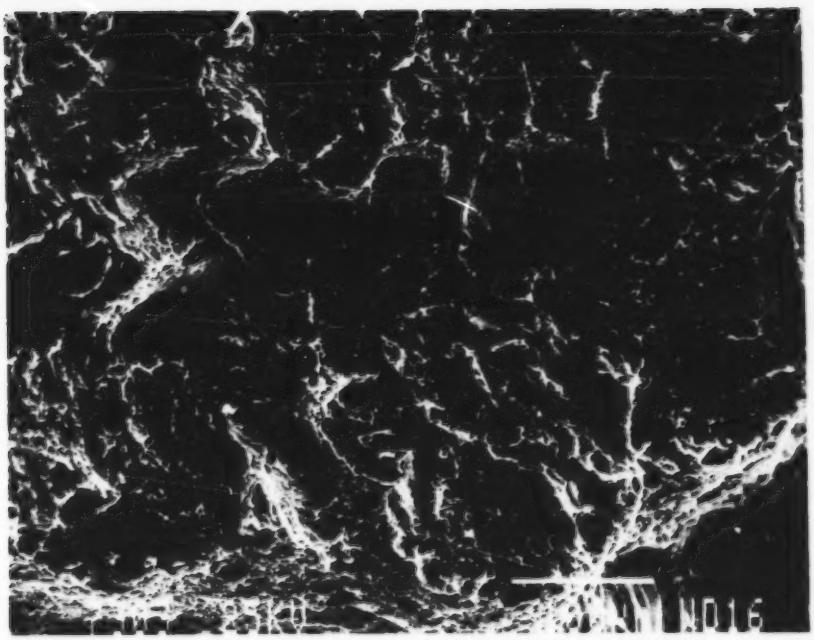

Figure 17 Fracture Appearance of Charpy Sample No. 73
Middle of Sample: Largely Cleavage
with Intergranular Fracture

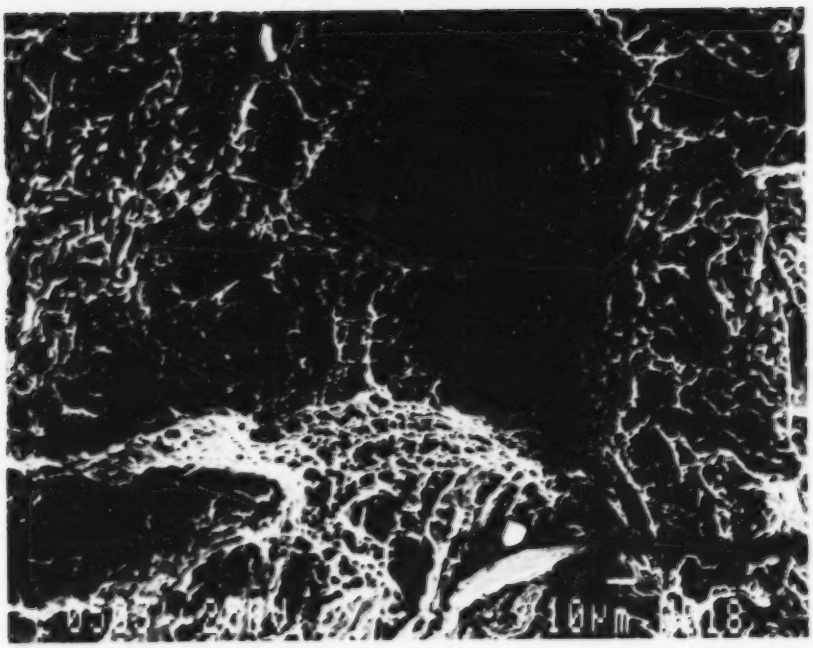

Figure 18 Fracture Appearance of Charpy Sample 10S Predominantly Ductile with Intergranular Patches

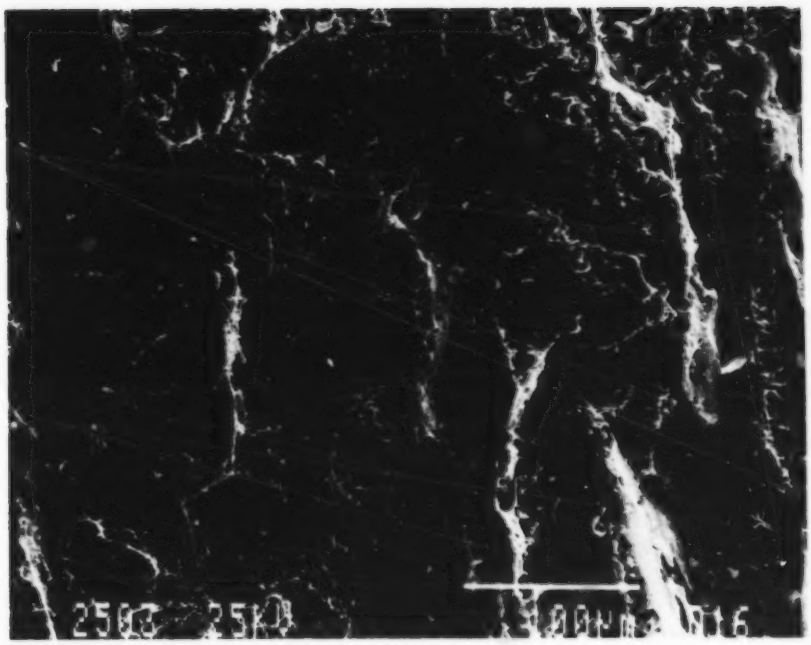

Figure 19 Fracture Appearance of Charpy Sample 12S
Intergranular and Cleavage
Fracture

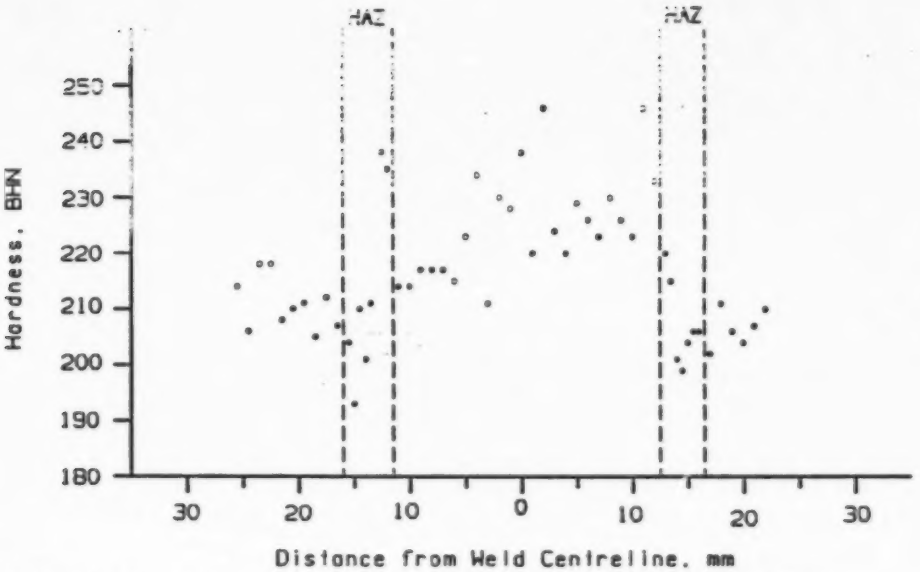

Figure 20 Microhardness Survey Across Circumferential Seam T/4 Location

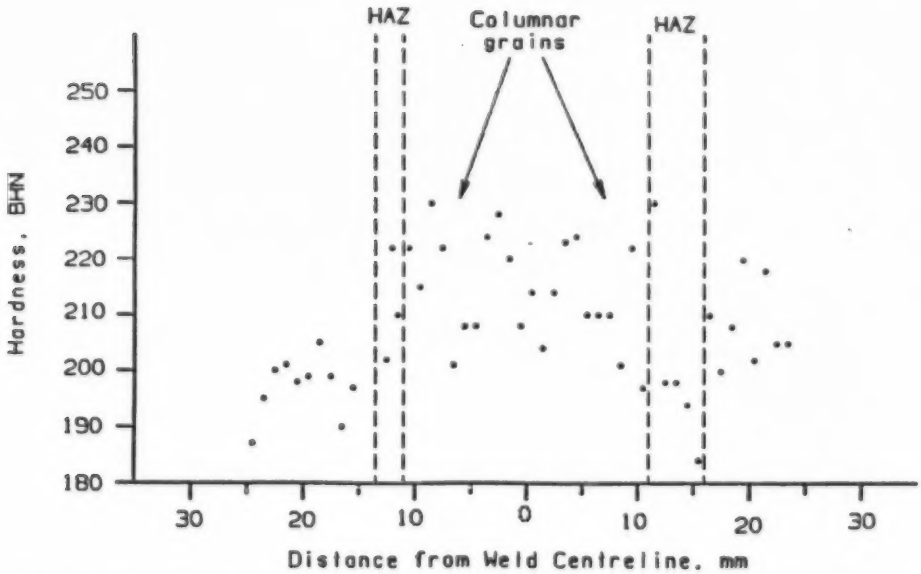

Figure 21 Microhardness Survey Across Circumferential Seam T/2 Location

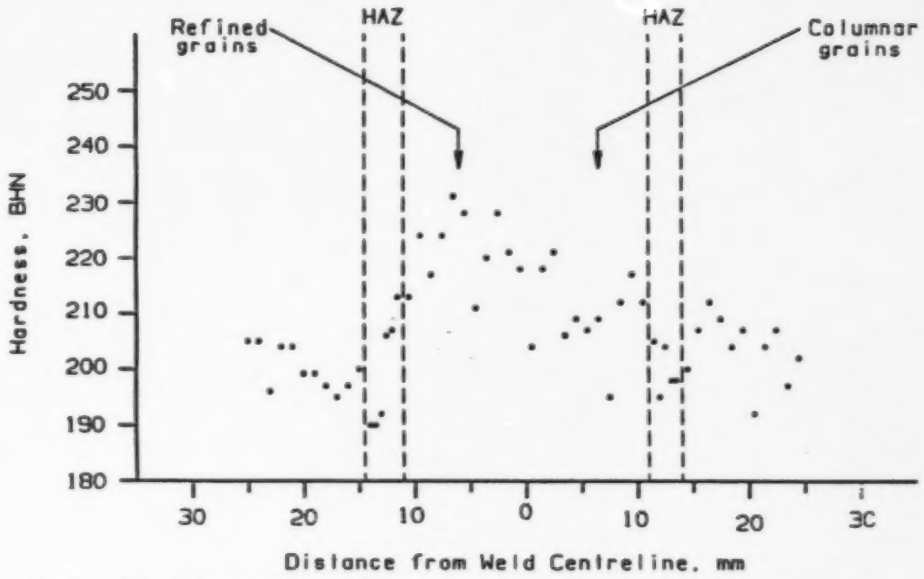

Figure 22 Microhardness Survey Across Circumferential Seam 3T/4 Location

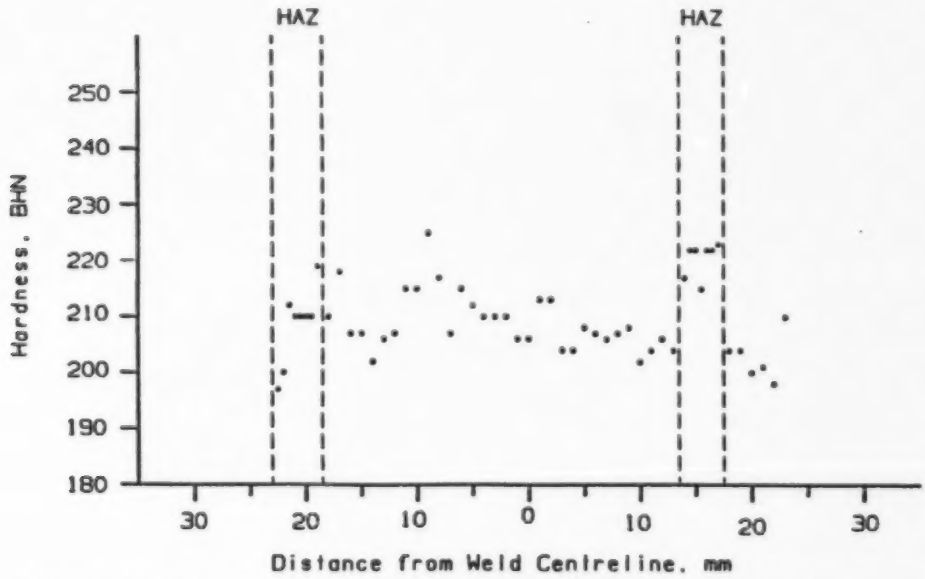

Figure 23 Microhardness Survey Across Circumferential 1.6 mm from Weld Root